Edinburgh Research Explorer

A Frequency Domain Approach to Eigenvalue-Based Detection with Diversity Reception and Spectrum Estimation

Link:
[Link to publication record in Edinburgh Research Explorer](#)

Document Version:
Peer reviewed version

Published In:
IEEE Transactions on Signal Processing

A Frequency Domain Approach to Eigenvalue-Based Detection with Diversity Reception and Spectrum Estimation

Ebtihal H. G. Yousif[1], *Member, IEEE,*

and Tharmalingam Ratnarajah[1], *Senior Member, IEEE*

and Mathini Sellathurai[2], *Senior Member, IEEE*

Abstract

In this paper, we investigate a frequency domain approach for eigenvalue-based detection of a primary user, based on equal gain combining (EGC) and spectrum estimation with Bartlett's method. This paper considers two techniques for eigenvalue detection which are Maximum Eigenvalue Detection (MED) and the Maximum-Minimum Eigenvalue (MME) detector. We exploit the eigenvalues that are associated with the Hermitian form representation of Bartlett's estimate to assess the performance of the aforementioned eigenvalue techniques in the frequency domain. For each case, we quantify the performance based on the probabilities of false alarm and missed detection over Rayleigh and Rician fading. A bivariate Mellin transform approach is employed to obtain the probability distribution function for the ratio of the extreme eigenvalues under each hypothesis. All obtained formulas are validated via Monte-Carlo simulations, and the results give a clear insight into the performance of the investigated methods. In frequency domain, MED outperforms both the MME detector and Periodogram-based energy

[1]Ebtihal Yousif and Tharmalingam Ratnarajah are with the Institute of Digital Communication (IDCOM), School of Engineering, The University of Edinburgh, Edinburgh, UK, e-mails: e.yousif@ed.ac.uk, t.ratnarajah@ed.ac.uk.

[2]Mathani Sellathurai is with the School of Engineering and Physical Sciences, Heriot-Watt University, Edinburgh, UK, e-mail: M.Sellathurai@hw.ac.uk

detection even in a worst case scenario of noise uncertainty, while the MME detector exhibits heavy-tailed statistical characteristics and thus its receiver operating characteristics tend to stay on the line of no-discrimination. The performance of MED is further enhanced by careful choice of combinations of the total length of the sensing frame and number of sub-slots.

Index Terms

Bartlett's method, bivariate Mellin transform, eigenvalue analysis, EGC, Hermitian quadratic forms, order statistics, spectrum sensing.

I. INTRODUCTION

Multiple antennas were shown to provide significant enhancement in the performance of wireless communications systems. A notable application is developing efficient detection techniques that enables opportunistic spectrum access (OSA), which is required for next generation technologies such as cognitive radio (CR) systems and Leased Shared Access (LSA). A CR network consists of license-exempt nodes that sense and exploit underused frequency spectrum. The phrases "*primary users (PUs)*" and "*secondary users (SUs)*" are coined to refer to original license owners and license-exempt users respectively. On the other hand, LSA is a new approach that allows *incumbents* (license owners) to share the spectrum with a limited number of LSA licensees [1]. In a specific region, such mode of operation is governed by the national regulatory agency (NRA) and the sharing agreement with the incumbents.

In general, sensing methods are categorized based on the characteristics of the signal to be detected [2]. Apart from the common detection methods of matched filtering, energy detection and cyclostationary feature detection (CFD), one particular method is eigenvalue detection [3]–[6]. The conventional approach for eigenvalue detection uses the eigenvalues of the sample covariance matrix. Methods of eigenvalue-based detection include: 1) maximum eigenvalue detection (MED); 2) maximum-minimum eigenvalue (MME) detection; 3) energy-with-minimum-eigenvalue (EME) detection; and 4) the generalized likelihood ratio test (GLRT). MED is investigated in [3], and both the EME and the MME detectors are considered in [4]. Also, using random matrix theory a cooperative spectrum sensing approach based on the MME detector was investigated in [5]. Taking into account the impact of noise uncertainty, a throughput analysis was conducted for the MME and MED methods in [7]. Finally, a sensing-throughput trade-off

was provided in [6], with a focus on EME and GLRT. It is also noteworthy that the analysis provided in all the aforementioned studies did not consider a frequency domain (FD) approach.

In this paper, we consider a new approach for eigenvalue detection in frequency domain using reception diversity and spectrum estimation. Previous work in frequency domain techniques was presented in [8] using Periodograms, and [9] for Bartlett's method, and [10] for Welch's method of segmented and overlapped averaging, and finally in [11] for the Multitaper method. Note that all the aforementioned previous work using spectrum estimation did not develop eigenvalue methods. In this paper, and since we focus on frequency domain, we exploit the eigenvalues that are associated with the spectrum estimate, which results from diagonalizing the Hermitian form representation of the spectrum estimate.

The contributions of this paper are explained as follows. Using multiple antennas and diversity reception with equal gain combining (EGC), we investigate the MED and the MME detectors in FD based on Bartlett's method. For both cases, the performance is quantified in terms of the probabilities of false alarm and missed detection. For the case of the MME detector, and due to correlation, a bivariate Mellin transform approach[1] is employed to derive the probability distribution function (PDF) of the ratio of extreme eigenvalues. Furthermore, a comparison is demonstrated between MED, the MME detector and Periodogram-based energy detection assuming a worst case scenario for noise uncertainty. It will be shown that in FD the MED detector yields the best performance even under noise uncertainty. On the other hand, it will be shown that the decision statistic for the MME detector has a right heavy tail which forces the receiver operating characteristic curves to lie on the line of no-discrimination. Further insight into the performance of the investigated detectors will be discussed over Rayleigh and Rician fading.

The rest of this paper is organized as follows. Section II presents the problem formulation. Section III, investigates direct estimation of the eigenvalues and their statistical attributes. The performance of MED is investigated in Section IV, and the MME detector is analyzed in Section V. The ergodic performance is investigated in Section VI over Rayleigh and Rician fading. In Section VII simulation results are provided, and finally Section VIII concludes the paper. Proofs for specific derivations are presented in the appendices.

---

[1]See [12]–[14] for the double Mellin integral technique for correlated variables.

II. PROBLEM FORMULATION

A. Mathematical Operators

The following notations will be used in this paper. All vectors will be represented by boldface lower case characters, and matrices will be denoted by uppercase boldface characters. $\mathbf{I}_a$ is the identity matrix with order a. The notation $\lambda_i(\mathbf{A})$ denotes the i-th eigenvalue of the square matrix $\mathbf{A}$, and the subscript will be omitted when $\mathbf{A}$ has rank one. The notation $\mathrm{diag}(a_1, \ldots, a_n)$ is a $n \times n$ diagonal matrix with diagonal elements $a_1, \ldots, a_n$.

The imaginary unit is j. The notations $(\cdot)^{\mathrm{T}}$ and $(\cdot)^{\dagger}$ denote the transpose and the conjugate transpose respectively. The notations $|\cdot|$, $\|\cdot\|_p$ and $\|\cdot\|_{\mathrm{F}}$ denote the magnitude operator, the p-norm and the Frobenius norm respectively. Finally the notation $^{+}|\cdot|^{+}$ denote the permanent of a matrix.

Any estimated parameter will be denoted by $\hat{(\cdot)}$. The notation $\bigoplus$ is the direct sum operator. The notation $\mathfrak{S}_n$ is a symmetric group on the finite set $\{1, \ldots, n\}$. The expectation operator is $\mathcal{E}\{\cdot\}$, $f_a(\cdot)$ is the PDF of the variable a, and the cumulative distribution function (CDF) of a will be denoted by $F_a(\cdot)$. The notation $\mathbb{EXP}(\cdot)$ denotes the exponential distribution, whereas both $\exp(\cdot)$ and $e^{(\cdot)}$ denote the exponential function.

Finally, the Mellin transformation of $g(x)$ into the variable $s \in \mathbb{C}$ will be denoted by $\mathcal{M}\{g(x); s\}$, and the inverse transformation is $\mathcal{M}^{-1}\{g(s); x\}$. The bivariate Mellin transform is $\mathcal{M}\{g(x, y); s_1, s_2\}$, and the corresponding inverse will be written as $\mathcal{M}^{-1}\{g(s_1, s_2); x, y\}$.

B. System Model

Let us consider the case of detecting a primary node that is equipped with a single antenna, using a secondary node equipped with N antenna branches. The output samples from all branches are assumed independent and identically distributed (i.i.d.). It is assumed that the sensing frame is of length M, with K sensing sub-slots, where each sub-slot contains m_{B} samples. At each time instant, EGC [2] is employed to combine the received samples from all branches. The resultant sequence of samples is used to estimate the eigenvalues of Bartlett's method of spectrum

---

[2]From a spectrum sensing point of view, maximum ratio combining (MRC) is not addressed in this paper since it is usually used within a cooperative spectrum sensing context (with reporting channels and a central data fusion center) and it requires the channel state information (CSI) from the primary node to the secondary user(s), and from each secondary user to the fusion center [15].

estimation. Hence, the estimated eigenvalues will be used as a test statistic to distinguish between the hypothesis $\mathcal{H}_0$ (the primary user is idle), and the alternate hypothesis $\mathcal{H}_1$ (the primary user is active).

Based on the aforementioned scenario, let $\mathbf{x}(t) \in \mathbb{C}^{N \times 1}$ denote the received signal by the secondary node at the t-th time instant. The hypothesis has the form

$$\mathcal{H}_0: \quad \mathbf{x}(t) = \boldsymbol{w}(t), \tag{1}$$

$$\mathcal{H}_1: \quad \mathbf{x}(t) = \mathbf{h}(t)s(t) + \boldsymbol{w}(t), \tag{2}$$

where $\mathbf{x}(t)$ has the form

$$\mathbf{x}(t) = \begin{bmatrix} x(1,t) \\ x(2,t) \\ \vdots \\ x(N,t) \end{bmatrix}, \quad t = 0, \dots, M-1. \tag{3}$$

and $\mathbf{h} \in \mathbb{C}^{N \times 1}$ and $\boldsymbol{\omega} \in \mathbb{C}^{N \times 1}$ denote the channel and the noise vectors respectively, which are defined as

$$\mathbf{h}(t) = \begin{bmatrix} h(1,t) & h(2,t) & \dots & h(N,t) \end{bmatrix}^{\mathrm{T}}, \tag{4}$$

$$\boldsymbol{\omega}(t) = \begin{bmatrix} \omega(1,t) & \omega(2,t) & \dots & \omega(N,t) \end{bmatrix}^{\mathrm{T}} \tag{5}$$

and $x(n,t)$ denotes the received signal by the n-th antenna at the t-th time instant, which is given by

$$\mathcal{H}_0: \quad x(n,t) = w(n,t), \tag{6}$$

$$\mathcal{H}_1: \quad x(n,t) = h(n,t)s(t) + w(n,t), \tag{7}$$

where $n = 1, 2, \dots, N$ and $t = 0, 1, \dots, M-1$. The notation $w(n,t)$ denote the instantaneous value of AWGN at the n-th receiving branch. The noise is assumed to be a circular symmetric complex Gaussian process with $\mathcal{E}\{|w(n,t)|^2\} = \sigma_w^2$. Also, the noise samples are assumed independent and identically distributed. The notation $s(t)$ denotes the instantaneous symbol transmitted by the primary user at the t-th time instant, such that $\mathcal{E}\{|s(t)|^2\} = \sigma_s^2$. Finally, $h(n,t)$ is the instantaneous channel from the primary node to the n-th receiving branch.

From a generic point of view, EGC has reduced implementation complexity compared with MRC (because of the weights requirements for MRC), and outperforms the selection combiner (SC) [16].

C. Diversity Combining and Spectrum Estimation

As stated before, the sensing frame consists of M samples and a number of K sub-slots, where each sub-slot consists of m_{B} samples. Henceforth, let us define the column vector $\mathbf{x}_{\mathrm{EGC}} \in \mathbb{C}^{M \times 1}$ that is received by the end of the sensing frame, where

$$\mathbf{x}_{\mathrm{EGC}} = \mathrm{vec}\left(\tilde{\mathbf{x}}_1, \ldots, \tilde{\mathbf{x}}_K\right), \tag{8}$$

where $\tilde{\mathbf{x}}_p \in \mathbb{C}^{m_{\mathrm{B}} \times 1}$ represent the output after diversity combining of the p-th sensing slot, i.e,

$$\tilde{\mathbf{x}}_p = \begin{bmatrix} \sum_{i=1}^N x(i, (p-1)m_{\mathrm{B}}) \\ \sum_{i=1}^N x(i, (p-1)m_{\mathrm{B}}+1) \\ \sum_{i=1}^N x(i, (p-1)m_{\mathrm{B}}+2) \\ \vdots \\ \sum_{i=1}^N x(i, pm_{\mathrm{B}}-1) \end{bmatrix}, \ p = 1, 2, \ldots, K. \tag{9}$$

In frequency domain, let $\mathfrak{f}$ denote the frequency index, where $\mathfrak{f} = 0, \ldots, m_{\mathrm{B}}-1$, and therefore the longer the sensing sub-slot, the larger the resolution. It is shown in [9], that Bartlett's estimate can be written as a positive semi-definite Hermitian quadratic form. In this case, after EGC the spectrum $\mathcal{S}(\mathfrak{f})$ can be estimated using Bartlett's method as

$$\widehat{\mathcal{S}}(\mathfrak{f}) = \mathbf{x}_{\mathrm{EGC}}^{\dagger} \mathbf{V}(\mathfrak{f})\, \mathbf{x}_{\mathrm{EGC}}, \tag{10}$$

$$= \frac{1}{K} \sum_{p=1}^K \tilde{\mathbf{x}}_p^{\dagger}\, \tilde{\mathbf{v}}(\mathfrak{f})\, \tilde{\mathbf{v}}^{\dagger}(\mathfrak{f})\, \tilde{\mathbf{x}}_p, \tag{11}$$

where $\mathbf{V}(\mathfrak{f}) \in \mathbb{C}^{M \times M}$ is defined as

$$\mathbf{V}(\mathfrak{f}) = \frac{1}{K} \bigoplus_{p=1}^K \tilde{\mathbf{v}}(\mathfrak{f})\tilde{\mathbf{v}}(\mathfrak{f})^{\dagger}, \tag{12}$$

and $\tilde{\mathbf{v}}(\mathfrak{f}) \in \mathbb{C}^{m_{\mathrm{B}} \times 1}$ is given by

$$\tilde{\mathbf{v}}(\mathfrak{f}) = \frac{1}{m_{\mathrm{B}}} \left[1, e^{-\frac{2\pi j}{m_{\mathrm{B}}}\mathfrak{f}}, \ldots, e^{-\frac{2\pi j}{m_{\mathrm{B}}}\mathfrak{f}(m_{\mathrm{B}}-1)}\right]^{\mathrm{T}}. \tag{13}$$

However, the PDF of a diagonalizable Hermitian quadratic form can be represented in terms of the eigenvalues that are associated with the quadratic form. In this case, the eigenvalues to be addressed are the eigenvalues of the product of the covariance matrix and the matrix of the Hermitian quadratic form [17]. Henceforth, let $\widehat{\mathbf{R}}_{\mathrm{EGC}}$ denote the sample covariance matrix

estimated from $\mathbf{x}_{\mathrm{EGC}}$, and let $\widehat{\mathbf{R}}_p$ be the sample covariance matrix associated with the p-th segment $\tilde{\mathbf{x}}_p$, where $p = 1, \ldots, K$. We have

$$\widehat{\mathbf{R}}_{\mathrm{EGC}} \triangleq \frac{1}{M} \mathbf{x}_{\mathrm{EGC}} \mathbf{x}_{\mathrm{EGC}}^{\dagger}, \tag{14}$$

$$\widehat{\mathbf{R}}_p \triangleq \frac{1}{m_{\mathrm{B}}} \tilde{\mathbf{x}}_p \tilde{\mathbf{x}}_p^{\dagger}. \tag{15}$$

The Hermitian form representation of the estimate $\widehat{\mathcal{S}}(\mathfrak{f})$ is a function of the eigenvalues of the product of covariance matrix $\widehat{\mathbf{R}}_{\mathrm{EGC}}$ and the matrix $\mathbf{V}(\mathfrak{f})$. It was shown in [9] that the rank of the aforementioned matrix product is K, and therefore there are K non-zero eigenvalues associated with this product. This is attributed to the fact that the covariance matrix has full rank, while the matrix of the Hermitian form, $\mathbf{V}(\mathfrak{f})$, has rank K. The p-th eigenvalue is given by

$$\lambda_p \left(\widehat{\mathbf{R}}_{\mathrm{EGC}} \mathbf{V}(\mathfrak{f}) \right) = \frac{1}{K} \lambda \left(\widehat{\mathbf{R}}_p \tilde{\mathbf{v}}(\mathfrak{f}) \tilde{\mathbf{v}}^{\dagger}(\mathfrak{f}) \right). \tag{16}$$

D. Noise Uncertainty

Let $\hat{\sigma}_w^2 = \varrho \sigma_w^2$ be the expected noise power due to noise uncertainty, where ϱ is the noise uncertainty factor. In dB, the factor ϱ is uniformly distributed within the interval $[-B, B]$ and usually B is limited by 2 dB [18], where the upper bound B is given by

$$B = \sup \{ 10 \log_{10} \varrho \}, \tag{17}$$

and hence the PDF of ϱ is given by

$$f_{\varrho}(z) = \begin{cases} \frac{5}{\log(B)z} & 10^{-0.1B} < z < 10^{0.1B}, \\ 0 & \text{elsewhere.} \end{cases} \tag{18}$$

Noise uncertainty occurs because of the varying nature of the noise variance as a function of time and/or location. Noise uncertainty is a challenging issue for spectrum sensing, because it affects the performance of detectors by imposing bounds that may make the detector extremely unreliable beyond specific values of the SNR [18].

III. ESTIMATION AND STATISTICAL ATTRIBUTES OF EIGENVALUES

In the subsequent parts of the paper we will follow the notations used in [19] and [20] for order statistics. The notation $\hat{\ell}_{(1)} \leq \ldots \leq \hat{\ell}_{(K)}$ will be used to denote the **ordered** eigenvalues, such that the maximum eigenvalue is $\hat{\ell}_{\max} = \hat{\ell}_{(K)}$ and the minimum eigenvalue is $\hat{\ell}_{\min} = \hat{\ell}_{(1)}$.

Henceforth, the **non-ordered** eigenvalues will be denoted as $\hat{\ell}_1, \ldots, \hat{\ell}_K$. Also, the PDF and the CDF of the r-th estimated eigenvalue are $f_{\hat{\ell}_r}$ and $F_{\hat{\ell}_r}$ respectively. For notational convenience and brevity we will use

$$f_r(z) = f_{\hat{\ell}_r}(z), \tag{19a}$$

$$F_r(z) = F_{\hat{\ell}_r}(z), \tag{19b}$$

$$f_{(r)}(z) = f_{\hat{\ell}_{(r)}}(z), \tag{19c}$$

$$F_{(r)}(z) = F_{\hat{\ell}_{(r)}}(z), \tag{19d}$$

where $r = 1, \ldots, K$. As a first step, we need to obtain direct formulas to estimate the eigenvalues which are associated with the spectrum estimate. First, since we know that the p-th eigenvalue is the eigenvalue associated with the p-th segment, then we can write

$$\lambda_p \left(\widehat{\mathbf{R}}_{\mathrm{EGC}} \mathbf{V}(\mathfrak{f}) \right) = \frac{1}{K} \mathrm{tr} \left(\widehat{\mathbf{R}}_p \tilde{\mathbf{v}}(\mathfrak{f})^\dagger \tilde{\mathbf{v}}(\mathfrak{f}) \right), \tag{20}$$

$$= \frac{1}{K} \tilde{\mathbf{v}}(\mathfrak{f})^\dagger \widehat{\mathbf{R}}_p \tilde{\mathbf{v}}(\mathfrak{f}). \tag{21}$$

Second, the result of the multiplication $\widehat{\mathbf{R}}_p \tilde{\mathbf{v}}(\mathfrak{f}) \tilde{\mathbf{v}}^\dagger(\mathfrak{f})$ is given by

$$\widehat{\mathbf{R}}_p \tilde{\mathbf{v}}(\mathfrak{f}) \tilde{\mathbf{v}}^\dagger(\mathfrak{f}) = \frac{1}{m_{\mathrm{B}}^2}$$

$$\times \begin{bmatrix} \sum_{i=0}^{m_{\mathrm{B}}-1} \sum_{p=1}^{N} \sum_{q=1}^{N} x(p,0)x(q,i)^\dagger e^{-\frac{2\pi}{m_{\mathrm{B}}}j\mathfrak{f}i} & \cdots & \sum_{i=0}^{m_{\mathrm{B}}-1} \sum_{p=1}^{N} \sum_{q=1}^{N} x(p,0)x(q,i)^\dagger e^{-\frac{2\pi}{m_{\mathrm{B}}}j\mathfrak{f}(i-m_{\mathrm{B}}+1)} \\ \sum_{i=0}^{m_{\mathrm{B}}-1} \sum_{p=1}^{N} \sum_{q=1}^{N} x(p,1)x(q,i)^\dagger e^{-\frac{2\pi}{m_{\mathrm{B}}}j\mathfrak{f}i} & \cdots & \sum_{i=0}^{m_{\mathrm{B}}-1} \sum_{p=1}^{N} \sum_{q=1}^{N} x(p,1)x(q,i)^\dagger e^{-\frac{2\pi}{m_{\mathrm{B}}}j\mathfrak{f}(i-m_{\mathrm{B}}+1)} \\ \vdots & \ddots & \vdots \\ \sum_{i=0}^{m_{\mathrm{B}}-1} \sum_{p=1}^{N} \sum_{q=1}^{N} x(p,m_{\mathrm{B}}-1)x(q,i)^\dagger e^{-\frac{2\pi}{m_{\mathrm{B}}}j\mathfrak{f}i} & \cdots & \sum_{i=0}^{m_{\mathrm{B}}-1} \sum_{p=1}^{N} \sum_{q=1}^{N} x(p,m_{\mathrm{B}}-1)x(q,i)^\dagger e^{-\frac{2\pi}{m_{\mathrm{B}}}j\mathfrak{f}(i-m_{\mathrm{B}}+1)} \end{bmatrix} \tag{22}$$

and then the estimated p-th eigenvalue is obtained as

$$\hat{\ell}_p = \frac{1}{K m_{\mathrm{B}}^2} \sum_{i=0}^{m_{\mathrm{B}}-1} \sum_{p=1}^{N} \sum_{q=1}^{N} \sum_{r=0}^{m_{\mathrm{B}}-1} x(p,r)x(q,i)^\dagger e^{-\frac{2\pi}{m_{\mathrm{B}}}j\mathfrak{f}(i-r)}. \tag{23}$$

Henceforth, considering the statistical properties of $\tilde{\mathbf{x}}_p$, it follows that

$$\mathcal{H}_0 : \tilde{\mathbf{x}}_p \sim \mathcal{CN}(0, N\sigma_w^2 \mathbf{I}_{m_{\mathrm{B}}}), \tag{24a}$$

$$\mathcal{H}_1 : \tilde{\mathbf{x}}_p \sim \mathcal{CN}(0, \sigma_s^2 \mathbf{3}_p \mathbf{3}_p^\dagger + N\sigma_w^2 \mathbf{I}_{m_{\mathrm{B}}}), \tag{24b}$$

where $\boldsymbol{3}_p \in \mathbb{C}^{m_{\mathrm{B}} \times m_{\mathrm{B}}}$ is defined as

$$\boldsymbol{3}_p = \mathrm{diag}\left(\sum_{i=1}^{N} h(i, (p-1)m_{\mathrm{B}}), \sum_{i=1}^{N} h(i, (p-1)m_{\mathrm{B}}+1), \right.$$
$$\left. \sum_{i=1}^{N} h(i, (p-1)m_{\mathrm{B}}+2), \ldots, \sum_{i=1}^{N} h(i, m_{\mathrm{B}}p-1) \right). \qquad (25)$$

Based on (23), and with the aid of [21] and [8], the p-th estimated eigenvalue is exponentially distributed as

$$\hat{\ell}_p \sim \begin{cases} \mathbb{EXP}\left(\dfrac{m_{\mathrm{B}}K}{N\sigma_w^2} \right), & \mathcal{H}_0, \\[4mm] \mathbb{EXP}\left(\dfrac{m_{\mathrm{B}}K}{N\sigma_w^2 + \frac{1}{m_{\mathrm{B}}}\|\boldsymbol{3}_p\|_{\mathrm{F}}^2 \sigma_s^2} \right), & \mathcal{H}_1, \end{cases} \qquad (26)$$

where $\boldsymbol{3}$ is given by (25).

IV. MAXIMUM EIGENVALUE DETECTION

The eigenvalues associated with a spectrum estimate can be used within the context of spectrum sensing, and this will be explained as follows. For example, at a given frequency index, when the primary user is absent then all of the eigenvalues of the quadratic form representation of the spectrum estimate are equivalent to $\frac{N\sigma_w^2}{m_{\mathrm{B}}K}$, i.e, $\ell_1 = \ldots = \ell_K = \frac{N\sigma_w^2}{m_{\mathrm{B}}K}$. However, when a primary user is present we have that $\ell_p > \frac{N\sigma_w^2}{m_{\mathrm{B}}K}$ for $p = 1, \ldots, K$. Hence, let us summarize the steps of maximum eigenvalue detection using the eigenvalues that are associated with Bartlett's estimate as follows:

- **Step 1:** Obtain the output of K successive sensing sub-slots, i.e., $\tilde{\mathbf{x}}_1, \ldots, \tilde{\mathbf{x}}_K$.
- **Step 2:** Estimate the covariance matrices $\widehat{\mathbf{R}}_1, \ldots, \widehat{\mathbf{R}}_K$.
- **Step 3:** Estimate the maximum eigenvalue using

$$\hat{\ell}_{\max} = \max\left\{ \frac{1}{K}\lambda_p\left(\widehat{\mathbf{R}}_{\mathrm{EGC}} \mathbf{V}(\mathfrak{f}) \right) \right\}_{p=1}^{K}. \qquad (27)$$

- **Step 4:** For a predetermined threshold η, apply the test

$$\hat{\ell}_{\max} \geq \eta, \qquad (28)$$

where the threshold is restricted by $\eta > \frac{N\sigma_w^2}{m_{\mathrm{B}}K}$.

Let us consider the null hypothesis $\mathcal{H}_0$. In this case, the estimated (but not ordered) eigenvalues are i.i.d., and the maximum estimated eigenvalue is the maximum of a number of K i.i.d.

exponential variables. Hence, based on the distribution parameters provided by (26), the PDF of the maximum estimated eigenvalue is given by

$$f_{\hat{\ell}_{\max}}(z; \mathcal{H}_0) = \frac{m_{\mathrm{B}} K^2}{\sigma_w^2 N} \exp\left(-\frac{m_{\mathrm{B}} K}{\sigma_w^2 N} z\right) \left[1 - \exp\left(-\frac{m_{\mathrm{B}} K}{\sigma_w^2 N} z\right)\right]^{K-1}. \tag{29}$$

By making use of the previous equation and for a given threshold η, the probability of false alarm is obtained as

$$P_{\mathrm{fa}}(\eta) = \mathrm{Prob}\left\{\hat{\ell}_{\max} \geq \eta \,|\, \mathcal{H}_0\right\} = 1 - \left[1 - \exp\left(-\frac{m_{\mathrm{B}} K}{\sigma_w^2 N} \eta\right)\right]^K. \tag{30}$$

On the other hand, when the channel is occupied by a primary user, the estimated (and not ordered) eigenvalues are independent but not identically distributed. Henceforth, let us define $\mathbf{f}$ and $\mathbf{F}$ as

$$\mathbf{f} = [f_1(.), \dots, f_K(.)], \tag{31}$$

$$\mathbf{F} = [F_1(.), \dots, F_K(.)]. \tag{32}$$

With the aid of [19], the PDF of the r-th ordered estimated eigenvalue is given by

$$f_{(r)}(z; \mathbf{f}, \mathbf{F}) = \frac{1}{(r-1)!(K-r)!} \begin{vmatrix} F_1(z) & \dots & F_K(z) \\ \vdots & & \vdots \\ F_1(z) & \dots & F_K(z) \\ f_1(z) & \dots & f_K(z) \\ 1 - F_1(z) & \dots & 1 - F_K(z) \\ \vdots & & \vdots \\ 1 - F_1(z) & \dots & 1 - F_K(z) \end{vmatrix}^+ \left.\begin{matrix} \\ \\ \end{matrix}\right\} r - 1 \text{ rows} \quad \left.\begin{matrix} \\ \\ \end{matrix}\right\} K - r \text{ rows} \tag{33}$$

Henceforth, based on the previous equation, the PDF of the estimated maximum eigenvalue is obtained as

$$f_{\hat{\ell}_{\max}}(z; \mathbf{f}, \mathbf{F}) = \sum_{\mathcal{G} \subset \mathfrak{S}_K} f_{g_1}(z) F_{g_2}(z) \dots F_{g_K}(z), \tag{34}$$

where the symmetric group $\mathfrak{S}_K$ contains all bijections from $\{1, \dots, K\}$ to itself, and the conjugacy classes are labeled as partitions of K. In this case, the subgroup $\mathcal{G}$ contains the K distinct permutations of the subscripts $g_1, \dots, g_K$. Hence, one can write

$$f_{\hat{\ell}_{\max}}(z; \mathbf{f}, \mathbf{F}) = \sum_{i=1}^{K} f_i(z) \prod_{p=1, p \neq i}^{K} F_p(z). \tag{35}$$

The cumulative distribution of the r-th order statistic is [20]

$$F_{(r)}(z; \mathbf{F}) = \sum_{i=r}^{K} \sum_{\mathcal{G}} \prod_{l=1}^{i} F_{g_l}(z) \prod_{l=i+1}^{K} 1 - F_{g_l}(z), \tag{36}$$

where $\mathcal{G}$ is the summation that extends over all the K distinct permutations $(j_1, \ldots, j_n)$ of $1, \ldots, K$. Hence, the CDF of the maximum estimated eigenvalue is

$$F_{\hat{\ell}_{\max}}(z; \mathbf{F}) = \prod_{i=1}^{K} F_i(z). \tag{37}$$

Therefore, the probability of missed detection is given by

$$P_{\mathrm{m}}(\eta) = \mathrm{Prob}\left\{\hat{\ell}_{\max} < \eta \,|\mathcal{H}_1\right\} = \prod_{p=1}^{K} 1 - \exp\left(\frac{-m_{\mathrm{B}} K \eta}{\sigma_w^2 N + \frac{1}{m_{\mathrm{B}}}\sigma_s^2 \|\mathbf{3}_p\|_{\mathrm{F}}^2}\right). \tag{38}$$

V. MAXIMUM-MINIMUM EIGENVALUE DETECTION

In this section the maximum-minimum eigenvalue detector is investigated and analyzed. In this case, the test statistic is the ratio of the maximum and the minimum estimated eigenvalues. However, as a consequence of ordering, the maximum and the minimum eigenvalues are correlated. Henceforth, let us use the notation

$$T_{\mathrm{MME}} = \frac{\hat{\ell}_{\max}}{\hat{\ell}_{\min}} = \frac{\hat{\ell}_{(K)}}{\hat{\ell}_{(1)}}. \tag{39}$$

to denote the test statistic. The steps of maximum-minimum eigenvalue detection can be summarized by the following steps.

- **Step 1:** Obtain the output of K successive sensing slots: $\tilde{\mathbf{x}}_1, \ldots, \tilde{\mathbf{x}}_K$.
- **Step 2:** Estimate the sample covariance matrices $\widehat{\mathbf{R}}_1, \ldots, \widehat{\mathbf{R}}_K$.
- **Step 3:** For each value of $\mathfrak{f}$, obtain the extreme eigenvalues:

$$\hat{\ell}_{\min} = \min\left\{\lambda_p\left(\frac{1}{K}\widehat{\mathbf{R}}_p\tilde{\mathbf{v}}(\mathfrak{f})\tilde{\mathbf{v}}^\dagger(\mathfrak{f})\right)\right\}_{p=1}^{K}, \tag{40}$$

$$\hat{\ell}_{\max} = \max\left\{\lambda_p\left(\frac{1}{K}\widehat{\mathbf{R}}_p\tilde{\mathbf{v}}(\mathfrak{f})\tilde{\mathbf{v}}^\dagger(\mathfrak{f})\right)\right\}_{p=1}^{K}. \tag{41}$$

- **Step 4:** Apply the test

$$\frac{\hat{\ell}_{\max}}{\hat{\ell}_{\min}} \geq \eta,$$

where $\eta > 1$.

A. PDF of the Ratio T_{MME} Under $\mathcal{H}_0$

In order to derive the probability distribution of T_{MME}, we need the joint PDF of the minimum and the maximum estimated eigenvalues $f_{(1),(K)}(z_{\min}, z_{\min})$. Let us start with the case of the null hypothesis $\mathcal{H}_0$. The PDF and the CDF of the minimum eigenvalue are given by

$$f_{(1)}(z; \mathcal{H}_0) = \frac{m_{\mathrm{B}}K^2}{N\sigma_w^2} \exp\left(-\frac{m_{\mathrm{B}}K^2}{N\sigma_w^2} z\right), \tag{42}$$

and

$$F_{(1)}(z; \mathcal{H}_0) = 1 - \exp\left(-\frac{m_{\mathrm{B}}K^2}{N\sigma_w^2} z\right) \tag{43}$$

respectively. On the other hand, considering the maximum estimated eigenvalue, the PDF is already given by (29) and then the CDF is

$$F_{(K)}(z; \mathcal{H}_0) = \left[1 - \exp\left(-\frac{m_{\mathrm{B}}K}{N\sigma_w^2} z\right)\right]^K. \tag{44}$$

Hence, with the aid of [22, Eq(3.4)], the joint PDF of the maximum and the minimum eigenvalues is obtained as

$$f_{(1),(K)}(z_{(1)}, z_{(K)}) = \frac{K!}{K-2!} f_{(1)}(z_{(1)}) f_{(K)}(z_{(K)}) \left[F_{(K)}(z_{(K)}) - F_{(1)}(z_{(1)})\right]^{K-2}, \tag{45}$$

Substituting equations (29), (42), (43) and (44) in (45) and applying the binomial theorem we arrive at

$$f_{\hat{\ell}_{\min}, \hat{\ell}_{\max}}\left(z_{(1)}, z_{(K)}; \mathcal{H}_0\right) = K! \left(\frac{m_{\mathrm{B}}K^2}{N\sigma_w^2}\right)^2 \exp\left(-\frac{m_{\mathrm{B}}K^2}{N\sigma_w^2} z_{(1)}\right) \exp\left(-\frac{m_{\mathrm{B}}K}{N\sigma_w^2} z_{(K)}\right)$$
$$\times \sum_{i=0}^{K-2} \frac{1}{i!\Gamma(K-i-1)} \left[1 - \exp\left(-\frac{m_{\mathrm{B}}K^2}{N\sigma_w^2} z_{(K)}\right)\right]^{Ki+K-1} \left[\exp\left(-\frac{m_{\mathrm{B}}K}{N\sigma_w^2} z_{(1)}\right) - 1\right]^{K-i-2} \tag{46}$$

where $\Gamma(\cdot)$ denotes the gamma function $\Gamma(n) = \int_0^\infty y^{n-1} e^{-y}\, dy$. Given a bivariate PDF, the statistical distributions of products and quotients of dependent random variables were investigated by [23], and reported by [24]. The derivation approach is based on the method that is employed for independent random variables [25] and the two dimensional Mellin integral [14], [26]. One result from the theorems presented by Fox in [14] can be summarized as follows.

Theorem *1 (PDF of Ratio of Correlated Variables):* Let U and V be positive and real random variables with bivariate PDF $f_{U,V}(u, v)$. The PDF of the ratio $Z = \frac{U}{V}$ can be obtained through the inverse Mellin transform of the double Mellin integral $\mathcal{M}\left[f_{U,V}(u, v); s_1, s_2\right]$ as

$$f_Z(z) = \mathcal{M}^{-1}\left\{\mathcal{M}\left\{f_{U,V}(u, v); s, 2-s\right\}; z\right\}. \tag{47}$$

Hence, using the joint PDF of the maximum and minimum eigenvalues obtained in (46), the PDF of the ratio of the maximum and minimum eigenvalues can be obtained using the inversion method of (47). The two dimensional Mellin transform of the joint PDF $f_{(1),(K)}(z_{(1)}, z_{(K)})$ into $\mathcal{G}(s_1, s_2)$ is

$$
\begin{aligned}
\mathcal{G}(s_1, s_2) =& \mathcal{M}\Big\{ f_{(1),(K)}(z_{(1)}, z_{(K)}); s_1, s_2 \Big\} \\
=& \int_0^\infty \int_0^\infty z_{(1)}^{s_1-1} z_{(K)}^{s_2-1} f_{(1),(K)}(z_{(1)}, z_{(K)}) \, \mathrm{d}z_{(1)} \mathrm{d}z_{(K)},
\end{aligned}
\tag{48}
$$

given that $z_{(1)} < z_{(K)}$.

Corollary *1:* The PDF of the ratio of the maximum and minimum estimated eigenvalues is given by

$$
\begin{aligned}
f_{\mathrm{MME}}(z) =& \frac{K!}{(K-2)!} \sum_{i=0}^{K-2} \sum_{c=0}^{Ki+K-1} \sum_{r=0}^{K-i-2} \\
&\times \left\{ \frac{1}{i!c!r!} \frac{\Gamma(K-1)\Gamma(K(i+1))}{\Gamma(K(i+1)-c)\Gamma(K-i-r-1)} (-1)^{K+c-r-i} \Big(K(1+r) + z(c+1) \Big)^{-2} \right\}.
\end{aligned}
\tag{49}
$$

Proof: The proof is provided in Appendix A. ∎

The cumulative distribution function can be derived by making use of (49), and then the probability of false alarm is obtained as follows.

Corollary *2:* The probability of false alarm for MME eigenvalue detection, based in Bartlett's method, is given by

$$
P_{\mathrm{fa}}(\eta) = K(K-1) \sum_{i=0}^{K-2} \sum_{c=0}^{Ki+K-1} \sum_{r=0}^{K-i-2} \frac{1}{i!} \frac{1}{c!} \frac{1}{r!} \frac{(-1)^K K^2 (1+c)^{-1} (K(1+r) + (1+c)\eta)^{-2}}{(1-K(i+1))_c (2-K+i)_r (2-K)_i}
\tag{50}
$$

where $(a)_b$ denotes Pochhammer's symbol.

Corollary *3:* The PDF of the ratio of the maximum and minimum estimated eigenvalues, given by (49), represents a heavy tailed distribution.

Proof: By making use of the result presented in Corollary 2, it is required to show that the limit of $e^{\kappa a} \mathrm{prob}[T_{\mathrm{MME}} > a]$ is infinity as $a \to \infty$, for $\kappa \in [0, \infty)$. Hence, applying L'Hôpital's

rule and after some manipulations we have that

$$
\lim_{a \to \infty} e^{\kappa a} \text{prob}[T_{\text{MME}} > a | \mathcal{H}_1]
$$

$$
= K(K-1)
$$

$$
\times \sum_{i=0}^{K-2} \sum_{c=0}^{Ki+K-1} \sum_{r=0}^{K-i-2} \left\{ \binom{K-2}{i} \binom{Ki+K-1}{c} \binom{K-i-2}{r} \frac{\kappa e^{\kappa a} K(-1)^{K-i+c-r}}{(c+1)(r+1)} \right\},
$$

$$
= \infty. \tag{51}
$$

Therefore, based on the previous result the moment generating function of the ratio of the maximum and the minimum eigenvalues is infinite as the corresponding PDF has a heavy right tail. ∎

B. PDF of the Ratio T_{MME} Under $\mathcal{H}_1$

In this part, we derive the PDF of the ratio of the maximum and the minimum eigenvalues assuming the alternate hypothesis $\mathcal{H}_1$. In this case, the ordered eigenvalues are independent, but not identically distributed as an impact of the time varying nature of the channel. To derive the joint PDF for this case, the PDF and the CDF of the maximum eigenvalue are already given by (35) and (37). However, expressions are required for the PDF and the CDF of the minimum eigenvalue which can be obtained as follows. By making use of the expression given by (33), the PDF of the minimum eigenvalue is obtained as

$$
f_{\hat{\ell}_{\min}}(z; \mathbf{f}, \mathbf{F}) = \frac{1}{(K-1)!} \left. \begin{vmatrix} f_1(z) & \dots & f_K(z) \\ 1 - F_1(z) & \dots & 1 - F_K(z) \\ \vdots & & \vdots \\ 1 - F_1(z) & \dots & 1 - F_K(z) \end{vmatrix}^+ \right\} K-1 \text{ rows} . \tag{52}
$$

After substituting the values of $f_i(z)$ and $F_i(z)$ for $i = 1, \dots, K$, the previous result can be reduced into a more convenient form. Hence, the PDF of the minimum eigenvalue can be rewritten as

$$
f_{\hat{\ell}_{\min} | \mathcal{H}_1}(z; \mathbf{f}, \mathbf{F}) = \sum_{i=1}^{K} \frac{m_{\text{B}} K}{\sigma_w^2 N + \frac{1}{m_{\text{B}}} \sigma_s^2 \|\mathbf{3}_i\|_{\text{F}}^2} \exp\left(-\sum_{p=1}^{K} \frac{m_{\text{B}} K z}{\sigma_w^2 N + \frac{1}{m_{\text{B}}} \sigma_s^2 \|\mathbf{3}_p\|_{\text{F}}^2} \right). \tag{53}
$$

The cumulative distribution can be obtained from (36), and thus we get

$$
F_{\hat{\ell}_{\min}}(z; \mathbf{F}) = \sum_{i=1}^{K} \sum_{\mathcal{G} \subset \mathfrak{S}_K} \prod_{l=1}^{i} F_{j_l}(z) \prod_{l=i+1}^{K} 1 - F_{j_l}(z). \tag{54}
$$

Next, given $\mathbf{f}$ and $\mathbf{F}$, the joint probability distribution function of the extreme order statistics is given by

$$
f_{\hat{\ell}_{\min},\hat{\ell}_{\max}}(z_{(1)}, z_{(K)}; \mathbf{f}, \mathbf{F})
$$

$$
= \frac{1}{(K-2)!}
\begin{vmatrix}
f_1(z_{(1)}) & \cdots & f_K(z_{(1)}) \\
F_1(z_{(K)}) - F_1(z_{(1)}) & \cdots & F_K(z_{(K)}) - F_K(z_{(1)}) \\
\vdots & \ddots & \vdots \\
F_1(z_{(K)}) - F_1(z_{(1)}) & \cdots & F_K(z_{(K)}) - F_K(z_{(1)}) \\
f_1(z_{(K)}) & \cdots & f_K(z_{(K)})
\end{vmatrix}
\left.\vphantom{\begin{matrix}a\\b\\c\end{matrix}}\right\} K-2 \text{ rows} \quad (55)
$$

However, equation (55) can be reduced into the summation:

$$
f\left(z_{(1)}, z_{(K)}; \mathbf{f}, \mathbf{F}\right) = \sum_{\mathcal{G} \subset \mathfrak{S}_K} f_{g_1}\left(z_{(1)}\right) \prod_{g_2 = g_1 + 1}^{g_3 - 1} F_{g_2}\left(z_{(K)}\right) - F_{g_2}\left(z_{(1)}\right) f_{g_3}\left(z_{(K)}\right), \quad (56)
$$

where summation is performed over all values of the subgroup $\mathcal{G}$ that consists of all the distinct permutations of the subscripts g_1, g_2, g_3. Thus, for this case every distinct term is counted $(K-2)!$ times, and hence the total number of summed elements is $K(K-1)$. Therefore, in the consequent subsections, only specific cases of K. Henceforth, let α_i denote the scale parameter that is associated with the PDF of the i-th non-ordered eigenvalue. For each investigated case of K, we will use Theorem 1 to derive the PDF of the ratio of the associated maximum and minimum eigenvalues using similar derivation steps to Appendix A.

1) K=2: The simplest case is having two sensing sub-slots. In this case, we have that $\mathcal{G} = \{\{1, 2\}, \{2, 1\}\}$ and from (55) the joint PDF can be rewritten as

$$
f\left(z_{(1)}, z_{(K)}\right) = \alpha_1 \exp\left(-\alpha_1 z_{(K)}\right) \alpha_2 \exp\left(-\alpha_2 z_{(1)}\right), + \alpha_1 \exp\left(-\alpha_1 z_{(1)}\right) \alpha_2 \exp\left(-\alpha_2 z_{(K)}\right), \quad (57)
$$

where α_i is given by

$$
\alpha_i = \frac{m_{\mathrm{B}} K}{\sigma_w^2 N + \frac{1}{m_{\mathrm{B}}} \sigma_s^2 \|\mathbf{3}_i\|_{\mathrm{F}}^2}. \quad (58)
$$

In order to derive the PDF of the ratio of the maximum and minimum eigenvalues using Theorem 1, let $\mathcal{G}_2(s_1, s_2)$ denote the double Mellin integral of the joint PDF when $K = 2$, and then we

get

$$
\mathcal{G}_2(s_1, s_2) = \mathcal{M}\left\{ f\left(z_{(1)}, z_{(2)} \right); s_1, s_2 \right\},
$$

$$
= s_1^{-1} \alpha_1 \alpha_2 (\alpha_1 + \alpha_2)^{-s_1 - s_2} \Gamma(s_1 + s_2)
$$

$$
\times \left\{ \frac{1}{s_1} {}_2F_1\left(1, s_1 + s_2; s_1 + 1; \frac{\alpha_2}{\alpha_1 + \alpha_2} \right) \frac{1}{s_2} {}_2F_1\left(1, s_1 + s_2; s_1 + 1; \frac{\alpha_1}{\alpha_1 + \alpha_2} \right) \right\}, \quad (59)
$$

where ${}_2F_1(.;.,.;.)$ is the Gaussian hypergeometric function and the strip of analyticity is defined as

$$
\left\{ (s_1, s_2) : \Re[s_1] > 0, \Re[s_2] > 0 \right\}.
$$

Similar to the same derivation procedure that is employed in Appendix A, the PDF of the ratio in this case is obtained as

$$
f(z) = \frac{1}{2\pi j} \frac{\alpha_1 \alpha_2}{(\alpha_1 + \alpha_2)^2}
$$

$$
\times \int_{\sigma - j\infty}^{\sigma + j\infty} \beta(2 - s, 1) \left[{}_2F_1\left(1, 2; 3 - s; \frac{\alpha_2}{\alpha_2 + \alpha_1} \right) + {}_2F_1\left(1, 2; 3 - s; \frac{\alpha_1}{\alpha_1 + \alpha_2} \right) \right] z^{-s} \, \mathrm{d}s
$$

$$
(60)
$$

where

$$
\sigma \in \left\{ s : 0 < \Re[s] < 2 \right\},
$$

and hence it can be easily obtained that

$$
f(z) = \frac{\alpha_1 \alpha_2}{(\alpha_2 + \alpha_1 z)^2} + \frac{\alpha_1 \alpha_2}{(\alpha_1 + \alpha_2 z)^2}. \quad (61)
$$

Using the previous result, the probability of missed detection is given by

$$
P_{\mathrm{m}}(\eta; \alpha_1, \alpha_2) = 1 - \frac{\alpha_2}{\alpha_2 + \alpha_1 \eta} - \frac{\alpha_1}{\alpha_1 + \alpha_2 \eta}. \quad (62)
$$

where α_i is given by (58).

2) K=3: When $K = 3$, then by making use of (55) the joint PDF can be written as

$$
f\left(z_{(1)}, z_{(K)}; K = 3 \right) = \sum_{\mathcal{G} \subset \mathfrak{S}_3} \alpha_{i_1} \exp\left(-\alpha_{i_1} z_{(K)} \right) \alpha_{i_2} \exp\left(-\alpha_{i_2} z_{(1)} \right) \exp\left(-\alpha_{i_3} z_{(1)} \right)
$$

$$
- \sum_{\mathcal{G} \subset \mathfrak{S}_3} \alpha_{i_1} \exp\left(-\alpha_{i_1} z_{(K)} \right) \alpha_{i_2} \exp\left(-\alpha_{i_2} z_{(1)} \right) \exp\left(-\alpha_{i_3} z_{(K)} \right), \quad (63)
$$

where the summation extends over all distinct permutations of the subscripts (i_1, i_2, i_3) of $(1, 2, 3)$. Using the previous result, the bivariate Mellin transform $\mathcal{G}_3(s_1, s_2) = \mathcal{M}\left\{ f(z_{(1)}, z_2); s_1, s_2 \right\}$ is given by

$$\mathcal{G}_3(s_1, s_2) = \sum_{\mathcal{G} \subset \mathfrak{S}_3} \frac{\alpha_{i_1} \alpha_{i_2} \Gamma(s_1 + s_2)}{s_1(\alpha_{i_1} + \alpha_{i_2} + \alpha_{i_3})^{s_1+s_2}} \left\{ {}_2F_1\left(1, s_1 + s_2; s_1 + 1; \frac{\alpha_{i_2} + \alpha_{i_3}}{\alpha_{i_1} + \alpha_{i_2} + \alpha_{i_3}}\right) \right.$$
$$\left. - {}_2F_1\left(1, s_1 + s_2; s_1 + 1; \frac{\alpha_{i_2}}{\alpha_{i_1} + \alpha_{i_2} + \alpha_{i_3}}\right) \right\}, \quad (64)$$

and applying Theorem 1 the PDF of the ratio is obtained by inverting $\mathcal{G}_3(s_1, s_2)$. We get

$$f(z) = \mathcal{M}^{-1}\left\{ \mathcal{M}\left\{ f(z_{(1)}, z_3); 2 - s, s \right\}; z \right\}$$
$$= \sum_{\mathcal{G} \subset \mathfrak{S}_3} \frac{\alpha_{i_1} \alpha_{i_2}}{(\alpha_{i_1} z + \alpha_{i_2} + \alpha_{i_3})^2} - \sum_{\mathcal{G} \subset \mathfrak{S}_3} \frac{\alpha_{i_1} \alpha_{i_2}}{(\alpha_{i_1} z + \alpha_{i_2} + \alpha_{i_3} z)^2}. \quad (65)$$

Thus, using the previous result, the probability of missed detection is obtained as

$$P_{\mathrm{m}}(\eta; \alpha_{i_1}, \alpha_{i_2}, \alpha_{i_3})$$
$$= 1 - \sum_{\mathcal{G}} \alpha_{i_2}\left(\alpha_{i_1}\eta + \alpha_{i_2} + \alpha_{i_3}\right)^{-1} + \sum_{\mathcal{G}} \alpha_{i_1}\alpha_{i_2}\left(\alpha_{i_1} + \alpha_{i_3}\right)^{-1}\left(\alpha_{i_1}\eta + \alpha_{i_2} + \alpha_{i_3}\eta\right)^{-1}. \quad (66)$$

3) K=4: When 4 sensing sub-slots are employed, the complexity of computing the permanent expression in (55) is increased, as the order of $\mathfrak{S}_K$ is $K!$. Hence, by making use of (55), and for a number of 4 sensing sub-slots the joint PDF of the maximum and the minimum eigenvalues is obtained as given by

$$f(z_{(1)}, z_{(K)}; \alpha_{i_1}, \alpha_{i_2}, \alpha_{i_3}, \alpha_{i_4})$$
$$= \sum_{\mathcal{G}} \alpha_{i_1} e^{-\alpha_{i_1} z_{(1)}} e^{-\alpha_{i_2} z_{(1)}} e^{-\alpha_{i_3} z_{(1)}} \alpha_{i_4} e^{-\alpha_{i_4} z_{(K)}} + \sum_{\mathcal{G}} \alpha_{i_1} e^{-\alpha_{i_1} z_{(1)}} e^{-\alpha_{i_2} z_{(K)}} e^{-\alpha_{i_3} z_{(K)}} \alpha_{i_4} e^{-\alpha_{i_4} z_{(K)}}$$
$$- \sum_{\mathcal{G}} \alpha_{i_1} e^{-\alpha_{i_1} z_{(1)}} e^{-\alpha_{i_2} z_{(1)}} e^{-\alpha_{i_3} z_{(K)}} \alpha_{i_4} e^{-\alpha_{i_4} z_{(K)}} - \sum_{\mathcal{G}} \alpha_{i_1} e^{-\alpha_{i_1} z_{(1)}} e^{-\alpha_{i_2} z_{(K)}} e^{-\alpha_{i_3} z_{(1)}} \alpha_{i_4} e^{-\alpha_{i_4} z_{(K)}},$$
$$(67)$$

and the bivariate Mellin transform is given by

$$
\mathcal{G}_4(s_1, s_2) = \frac{\Gamma(s_1 + s_2)}{\sum_{n=1}^{4} \alpha_n}
$$

$$
\times \sum_{\mathcal{G} \subset \mathfrak{S}_4} \alpha_{i_1} \alpha_{i_4} \left\{ {}_2F_1\left(1, s_1 + s_2; s_1 + 1; \frac{\alpha_{i_1} + \alpha_{i_2}}{\sum_{n=1}^{4} \alpha_n}\right) + {}_2F_1\left(1, s_1 + s_2; s_1 + 1; \frac{\alpha_{i_1} + \alpha_{i_3}}{\sum_{n=1}^{4} \alpha_n}\right) \right.
$$

$$
\left. - {}_2F_1\left(1, s_1 + s_2; s_1 + 1; \frac{\sum_{i=1}^{3} \alpha_i}{\sum_{n=1}^{4} \alpha_n}\right) - {}_2F_1\left(1, s_1 + s_2; s_1 + 1; \frac{\alpha_{i_1}}{\sum_{n=1}^{4} \alpha_n}\right) \right\}.
$$

$$(68)$$

Finally inverting $\mathcal{G}_4(s_1, s_2)$ into $f(z)$ yields

$$
f(z; \alpha_{i_1}, \alpha_{i_2}, \alpha_{i_3}, \alpha_{i_4})
$$

$$
= \sum_{\mathcal{G} \subset \mathfrak{S}_4} \alpha_{i_1} \alpha_{i_4} \left(\alpha_{i_1} + \alpha_{i_2} + \alpha_{i_3} + \alpha_{i_4} z\right)^{-1} + \sum_{\mathcal{G} \subset \mathfrak{S}_4} \alpha_{i_1} \alpha_{i_4} \left(\alpha_{i_1} + (\alpha_{i_2} + \alpha_{i_3} + \alpha_{i_4}) z\right)^{-1}
$$

$$
- \sum_{\mathcal{G} \subset \mathfrak{S}_4} \alpha_{i_1} \alpha_{i_4} \left(\alpha_{i_1} + \alpha_{i_2} + (\alpha_{i_3} + \alpha_{i_4}) z\right)^{-1} - \sum_{\mathcal{G} \subset \mathfrak{S}_4} \alpha_{i_1} \alpha_{i_4} \left(\alpha_{i_1} + \alpha_{i_3} + (\alpha_{i_1} + \alpha_{i_2}) z\right)^{-1}.
$$

$$(69)$$

Hence, by making use of the previous result the probability of missed detection is given by

$$
P_{\mathrm{m}}(\eta; \alpha_{i_1}, \alpha_{i_2}, \alpha_{i_3}, \alpha_{i_4}) = 1 - \sum_{\mathcal{G} \subset \mathfrak{S}_4} \left\{ \frac{\alpha_{i_1}}{\alpha_{i_1} + \alpha_{i_2} + \alpha_{i_3} + \alpha_{i_4} z} + \frac{\alpha_{i_1} \alpha_{i_4} (\alpha_{i_2} + \alpha_{i_3} + \alpha_{i_4})^{-1}}{\alpha_{i_1} + (\alpha_{i_2} + \alpha_{i_3} + \alpha_{i_4}) z} \right.
$$

$$
\left. - \frac{\alpha_{i_1} \alpha_{i_4} (\alpha_{i_3} + \alpha_{i_4})^{-1}}{\alpha_{i_1} + \alpha_{i_2} + (\alpha_{i_3} + \alpha_{i_4}) z} - \frac{\alpha_{i_1} \alpha_{i_4} (\alpha_{i_1} + \alpha_{i_2})^{-1}}{\alpha_{i_1} + \alpha_{i_3} + (\alpha_{i_1} + \alpha_{i_2}) z} \right\}.
$$

$$(70)$$

VI. ERGODIC PERFORMANCE OVER RAYLEIGH AND RICIAN FADING

In this part, the average probability of missed detection is investigated for propagation over Rayleigh and Rician fading, and the theoretical bounds are provided for the average probabilities.

A. MED

1) Rayleigh Fading: Let us assume that the channel magnitude from the transmitting node to the n-th antenna branch is Rayleigh distributed, where $\mathbb{Var}\left[\|h(n, t)\|\right] = \Omega$. Considering MED, it can be shown via Jensen's inequality that the average probability of missed detection is bounded by

$$
\mathcal{E}\left\{P_{\mathrm{m}}(\eta; \mathbf{3}_1, \ldots, \mathbf{3}_K)\right\} \leq \left(1 - \exp\left(\frac{-m_{\mathrm{B}} K \eta}{N(\sigma_w^2 + \sigma_s^2 \Omega)}\right)\right)^K.
$$

$$(71)$$

2) Rician Fading: Let us assume that the channel magnitude is a Rician process, where $\mathcal{E}\{|h(n,t)|\} = \mu_h$ and $\mathbb{V}\mathrm{ar}\,[|h(n,t)|] = \sigma_h^2$. Hence, it also follows that $\mathcal{E}\left\{\|\mathbf{3}_p\|_{\mathrm{F}}\right\}$ and $\mathcal{E}\left\{\|\mathbf{3}_p\|_{\mathrm{F}}^2\right\}$ are given by

$$\mathcal{E}\left\{\|\mathbf{3}_p\|_{\mathrm{F}}\right\} = 0.5 m_{\mathrm{B}} \sigma_h \sqrt{\pi N} L_{\frac{1}{2}}\left(\frac{-N\nu^2}{\sigma_h^2}\right) \tag{72}$$

and

$$\mathcal{E}\left\{\|\mathbf{3}_p\|_{\mathrm{F}}^2\right\} = N^2 |\mu_h|^2 m_{\mathrm{B}} + N\sigma_h^2 m_{\mathrm{B}}\left(1 - \frac{\pi}{4}\left(L_{\frac{1}{2}}\left(\frac{-|\mu_h|^2 N}{\sigma_h^2}\right)\right)^2\right), \tag{73}$$

respectively, where $L_a(\cdot)$ is the Laguerre polynomial and

$$L_{1/2}(a) = e^{\frac{a}{2}}\left[(1-a)\,I_0\left(-\frac{a}{2}\right) - a I_1\left(-\frac{a}{2}\right)\right] \tag{74}$$

where $I_n(y) = \sum_{m=0}^{\infty}\frac{1}{m!\Gamma(m+n+1)}\left(\frac{y}{2}\right)^{2m+n}$ denotes the n-th order modified Bessel function of the second kind. Considering MED, the average probability of missed detection is bounded by

$$\mathcal{E}\left\{P_{\mathrm{m}}(\eta; \mathbf{3}_1, \ldots, \mathbf{3}_K)\right\} \leq \left[1 - \exp\left(\frac{-m_{\mathrm{B}} K \eta}{N\sigma_w^2 + N\sigma_h^2 \sigma_s^2 + N^2 |\mu_h|^2 \sigma_s^2}\right)\right]^K. \tag{75}$$

B. MME Detection

Considering the MME detector, the average eigenvalue is independent of the channel variations. In this case, it can be shown that the theoretical bounds for the average probability of missed detection are

$$\mathcal{E}\left\{P_{\mathrm{m}}(\eta; K=2)\right\} \leq \frac{\eta-1}{\eta+1}, \tag{76}$$

$$\mathcal{E}\left\{P_{\mathrm{m}}(\eta; K=3)\right\} \leq \frac{2(\eta^2 - 2\eta + 1)}{(2\eta+1)(\eta+2)}, \tag{77}$$

$$\mathcal{E}\left\{P_{\mathrm{m}}(\eta; K=4)\right\} \leq \frac{3(\eta^3 - 3\eta^2 + 3\eta - 1)}{(3\eta+1)(\eta+3)(\eta+1)}. \tag{78}$$

VII. SIMULATION RESULTS AND DISCUSSION

In this section we provide some numerical results to evaluate the performance of the investigated detectors. We verify the accuracy of the obtained formulas for the maximum eigenvalue detector and the maximum-minimum eigenvalue detector. Also, we provide further simulation results to give a deeper insight into the performance of both detectors. For Monte-Carlo simulations, the results are averaged over 10^5 realizations.

A. The MED Detector

Fig.1 illustrates the complementary receiver operating characteristic curves for the maximum eigenvalue detector. The figure depicts the average probability of missed detection versus the probability of false alarm for various values of the number of receiving branches N, assuming propagation over Rayleigh and Rician fading. Lines represent theoretical results, and symbols represent Monte-Carlo simulations. The simulation parameters are $M = 16$, $K = 2$, $\sigma_s^2 = -3$dB, $\sigma_w^2 = 0$dB and $|\mu_h|^2 = 13$. As the number of receiving branches increases, the probability of miss is reduced assuming propagation over Rician fading. However, as it can be seen from the figure, the case of propagation over Rayleigh fading seems to be immune to variations in the number of receiving branches. This is mathematically justified by looking into the expression of the theoretical bound given by (71), which shows that only significant variations of K, the number of sub-slots, can produce a change in the average probability of miss[3]. This can be attributed to:

$$\left(1 - \exp\left(\frac{-m_{\mathrm{B}}K\eta}{N(\sigma_w^2 + \sigma_s^2\Omega)}\right)\right)^K \approx \exp\left(-K\exp\left(-\frac{m_{\mathrm{B}}K\eta}{N(\sigma_w^2 + \sigma_s^2\Omega)}\right)\right). \tag{79}$$

However, as the number of sub-slots becomes large enough, i.e., $K \to \infty$, the average probability of miss is increased, i.e., $\mathcal{E}\{P_{\mathrm{m}}\} = 1$.

Fig.2 demonstrates the impact of varying the number of sub-slots K, for a fixed value of M. The figure depicts the complementary receiver operating characteristics for several cases of the number of sensing sub-slots over Rayleigh and Rician fading. The parameters used for simulation are $M = 1024$, $N = 4$, $\sigma_w^2 = 0$dB, $\sigma_s^2 = -6$dB and $|\mu_h|^2 = 4$. It can be seen that the performance is enhanced as the number of sensing sub-slots is increased when the SNR (per branch) is enhanced for fixed M.

In fact, looking at the structure of the maximum eigenvalue detector, it can be seen that it is analogous to choosing the maximum of several Periodograms, except that in this case the Periodograms are scaled with a factor that contains the number of sensing sub-slots. Therefore, increasing the total number of samples per sensing frame should not interfere with the performance of the detector. On the other hand, increasing the number of sensing sub-slots for a fixed length of the sensing frame will provide further improvement in the performance of the detector.

---

[3]When K is varied and all other parameters are fixed, or only K and N are varied simultaneously.

B. The MME Detector

In Fig.3 we illustrate the heavy-tailed behavior of the maximum-minimum eigenvalue detector based on Bartlett's method. The three sub-figures demonstrate the heavy tail of the PDF as the upper value of the samples is limited by $z = 10^3$ for the first case in Fig.3a, $z = 10^{10}$ for the second case in Fig.3b and $z = 10^{20}$ for the third case in Fig.3c. As shown in Corollary 3, the PDF of the ratio of the maximum and the minimum eigenvalues exhibits a heavy right tail. As a consequence, there will be an absence of positive exponential moments , i.e., the moment generating function will be infinite for all values larger than zero.

In Fig.4, the obtained formulas for the probabilities of false alarm and missed detection are verified. The figure illustrates the receiver operating characteristic curves, i.e., $P_{\mathrm{d}} \triangleq 1 - P_{\mathrm{m}}$ versus P_{fa}. The results are obtained using 3 receiving branches, $M = 96$, $K = \{2, 3, 4\}$, $\sigma_w^2 = 10$dB, $\sigma_s^2 = 0$dB, $\sigma_h^2 = 3$dB and $|\mu_h|^2 = 18$. The figure compares between: the results from Monte-Carlo simulation, the theoretical averages of the expressions obtained in Section V-B and the theoretical bounds obtained in Section VI. For the case of $K = 3$, the summation subgroup $\mathcal{G}$ for (66) is given by

$$\mathcal{G} = \Big\{ \{1, 2, 3\}, \{2, 1, 3\}, \{2, 3, 1\},$$
$$\{3, 2, 1\}, \{1, 3, 2\}, \{3, 2, 1\} \Big\}. \tag{80}$$

Using 4 sensing sub-slots, the subgroup $\mathcal{G} \subset \mathfrak{S}_4$ for the sum required in (70) is given by

$$\mathcal{G} = \Big\{ \{3, \{1, 2\}, 4\}, \{4, \{1, 2\}, 3\}, \{2, \{1, 3\}, 4\},$$
$$\{4, \{1, 3\}, 2\}, \{2, \{1, 4\}, 3\}, \{2, \{1, 4\}, 3\},$$
$$\{1, \{2, 3\}, 4\}, \{4, \{2, 3\}, 1\}, \{1, \{2, 4\}, 4\},$$
$$\{3, \{2, 4\}, 1\}, \{1, \{3, 4\}, 2\}, \{2, \{3, 4\}, 1\} \Big\}. \tag{81}$$

It is obvious that the theoretical models are accurate. However, due to the heavy tailed characteristics of the PDF of the ratio of the extreme eigenvalues the ROC curves tend to lie on the line of no-discrimination.

Fig.5 illustrates a comparison between the MED and the MME methods for various values of the length of the sensing frame and fixed number of sub-slots. The simulation parameters are $K = 32$, $\sigma_w^2 = 2$dB, $\sigma_s^2 = -3$dB, $\sigma_h^2 = 1.76$dB, $|\mu_h|^2 = 2$ for $M = \{256, 1024, 2048\}$.

The figure shows the results based on both Rayleigh and Rician fading. Note that the curves of Rician fading for the MME method are identical to the results from Rayleigh fading, and therefore omitted from the figure for brevity. Generally, the MED method is also immune to variation of M when the number of segments is fixed.

C. Comparison with Periodogram-based ED and Impact of Noise Uncertainty

Assuming that a single Periodogram is used, and assuming noise uncertainty and by making use of the results of [8] the probability of false alarm and the probability of detection are given by

$$P_{\text{fa}}(\eta, \varrho) = \mathcal{E}\left\{\exp\left(\frac{-\eta}{\varrho\sigma_w^2 N}\right)\right\}, \tag{82}$$

and

$$P_{\text{d}}(\eta, \varrho) = \mathcal{E}\left\{\exp\left(\frac{-\eta}{\varrho\sigma_w^2 N + \frac{\sigma_s^2}{NM}\sum_{q=0}^{M-1}\left|\sum_{p=1}^{N}h(p,q)\right|^2}\right)\right\}, \tag{83}$$

respectively, where

$$\min(P_{\text{d}}(\eta, \varrho)) = \begin{cases} \exp\left(\frac{-\eta}{N(\varrho\sigma_w^2 + \sigma_s^2\sigma_h^2)}\right), & \text{Rayleigh,} \\ \exp\left(\frac{-\eta}{N(\varrho\sigma_w^2 + \sigma_s^2\sigma_h^2 + N|\mu_h|^2)}\right), & \text{Rician.} \end{cases} \tag{84}$$

Considering the MED detector, the probability of false alarm and the probability of detection will be affected by noise uncertainty. The probability of false alarm is

$$P_{\text{fa}}(\eta, \varrho) = \mathcal{E}\left\{1 - \left[1 - \exp\left(-\frac{m_{\text{B}}K}{\varrho\sigma_w^2 N}\eta\right)\right]^K\right\}, \tag{85}$$

and the probability of missed detection is

$$P_{\text{m}}(\eta, \varrho) = \mathcal{E}\left\{\prod_{p=1}^{K} 1 - \exp\left(-\frac{m_{\text{B}}K}{\varrho\sigma_w^2 N + \frac{1}{m_{\text{B}}}\sigma_s^2\|\mathbf{3}_p\|_{\text{F}}^2}\eta\right)\right\}. \tag{86}$$

Considering the MME detector, and looking into the probability of false alarm given by (50), and looking into the results for the probability of missed detection that are given by (62) for the

case of $K = 2$, (66) for $K = 3$ and (70) for $K = 4$, it is obvious that the MME detector is not affected by noise uncertainty.

Assuming propagation over Rayleigh fading, Fig.6 shows a comparison between the maximum eigenvalue detector and the Periodogram. The results shown in the figure assume a worst case of noise uncertainty when the factor ϱ is limited by $B = 2\text{dB}$[4]. The simulation parameters are $N = 4$, SNR $= \{0, -4\}$ (dB). For the MED detector it is assumed that $M = 1024$ and $K = 16$. The periodogram was simulated for $M = 64$. Similarly, Fig.7 provides the performance comparison under noise uncertainty but assuming Rician fading. The simulation parameters are $B = 2\text{dB}$, $\sigma_s^2 = \{-10, -20\}$ (dB), $M = 1024$, $K = 32$, $\mathbb{E}[|\mu_h^2|^2] = 4.5$. Another example is provided for the periodogram using a sample size of 64. In both figures (Fig.6 andFig.7), the MED method outperforms periodogram based ED. It is worthy to mention that the periodogram is immune to changes on samples size (this is illustrated by simulating the periodogram for both $M = 1024$ and $M = 64$). On the other hand careful choice of combinations of sample size and number of segments provides enhanced performance by the MED detector.

VIII. CONCLUSION

In this study, the aim is to assess the applicability of FD-based eigenvalue detection with Bartlett's power spectral estimator. The considered scenario consists of a sensing node equipped with multiple antennas and diversity combining with EGC. Two classes of the eigenvalue detector are investigated, which are MED and the MME detector. The results confirmed that the analytical models for the performance measures are accurate, and generally MED performs better than the MME detector in FD, even when taking noise uncertainty into account. Furthermore, the performance of MME can be controlled by the size of the sensing frame and the corresponding number of sensing sub-slots. On the other hand, it is shown that the PDF associated with the decision statistic of the MME detector exhibits a heavy right tail. Therefore, although this detector is immune to noise uncertainty, it always tends to balance between the probabilities of false alarm and missed detection such that the receiver operating characteristics lies on the line of no-discrimination.

---

[4]The noise uncertainty factor of a receiver is from 1 to 2 dB [27].

APPENDIX A

PDF OF THE RATIO OF THE MAXIMUM AND MINIMUM EIGENVALUES ASSUMING $\mathcal{H}_0$

In order to obtain the PDF of the ratio of the maximum and the minimum eigenvalues, let us start with the joint PDF given by (55). With the aid of [28, Sec. 1.3] and [29, Sec. 6.455], the bivariate Mellin transform of the joint PDF is obtained as

$$
\begin{aligned}
\mathcal{G}(s_1, s_2) &= \mathcal{M}\left\{ f\left(z_{(1)}, z_{(K)}\right); s_1, s_2 \right\} \\
&= \frac{K!}{(K-2)!} \sum_{i=0}^{K-2} \sum_{c=0}^{Ki+K-1} \sum_{r=0}^{K-i-2} \left\{ \frac{1}{i!}\frac{1}{c!}\frac{1}{r!} \frac{\Gamma(K-1)\Gamma(K(i+1))}{\Gamma(K(i+1)-c)\Gamma(K-i-r-1)} \right. \\
&\qquad \times K^2 (-1)^{K-2-i-r} \frac{\Gamma(s_1+s_2)}{\left(K(r+1)+(c+1)\right)^{s_1+s_2}} \\
&\qquad \left. \times {}_2F_1\left(s_2, s_1+s_2; s_2+1; \frac{K(r+1)}{K(r+1)+(c+1)}\right)\right\}, \quad (87)
\end{aligned}
$$

where ${}_2F_1(.;.;.)$ is the Gaussian hypergeometric function. In this case, the *strip of analyticity* (SOA) that is associated with the previous equation is the strip that is defined by the conditions

$$
\begin{cases}
\Re[s_1] > 0, \\
\Re[s_2] > 0, \\
\frac{(p+1)N\sigma_w^2}{m_{\mathrm{B}}K} > 0, \\
\frac{m_{\mathrm{B}}K}{N\sigma_w^2}\left(p+1+(r+1)K\right) \geq 0, \\
\Re[s_1+s_2] < 1 \text{ or } \frac{m_{\mathrm{B}}K}{N\sigma_w^2}\left(p+1+(r+1)K\right) > 0.
\end{cases} \quad (88)
$$

By applying [24, Theorem 4.8.2], the PDF of the ratio of $z_{(K)}$ and $z_{(1)}$ can be obtained by the inverse Mellin integral that is given by

$$
f(z) = \frac{1}{2\pi j} \int_{\sigma-j\infty}^{\sigma+j\infty} z^{-s} \mathcal{M}\left\{ f\left(z_{(1)}, z_{(K)}\right); s, 2-s \right\} \mathrm{d}s, \quad (89)
$$

where $\sigma \in \mathbb{R}$ lies within the associated strip of analyticity, and we obtain the integral given by

$$
\begin{aligned}
f(z) &= \frac{K!}{(K-2)!} \sum_{i=0}^{K-2} \sum_{c=0}^{Ki+K-1} \sum_{r=0}^{K-i-2} \\
&\quad \times \left\{ \frac{1}{i!}\frac{1}{r!}\frac{1}{c!} \frac{\Gamma(K-1)\Gamma(K(i+1))}{\Gamma(K(i+1)-c)\Gamma(K-i-r-1)} \frac{(-1)^{K-r-i+c}}{(K(r+1)+(c+1))^2} \right. \\
&\qquad \left. \times \frac{K^2}{2\pi j} \int_{\sigma-j\infty}^{\sigma+j\infty} z^{-s} \beta(2-s,1)\, {}_2F_1\left(1,2;3-s;\frac{K(r+1)}{K(r+1)+(c+1)}\right) \mathrm{d}s \right\}, \quad (90)
\end{aligned}
$$

where $\beta(\cdot,\cdot)$ denotes the beta function (the Euler integral of the first kind). By taking advantage of the relation

$$\mathcal{M}^{-1}\left\{\mathcal{G}(2-s);z\right\} = \frac{1}{z^2}\mathcal{M}^{-1}\left\{\mathcal{G}(s);\frac{1}{z}\right\},$$

and making use of [30, Sec. 7.5,(16)] we get

$$f(z) = \frac{K!}{(K-2)!}\sum_{i=0}^{K-2}\sum_{c=0}^{Ki+K-1}\sum_{r=0}^{K-i-2}\frac{1}{i!}\frac{1}{c!}\frac{1}{r!}$$

$$\times\left\{\frac{\Gamma(K-1)\Gamma(K(i+1))K^2(-1)^{K-2-i-r}}{\Gamma(K(i+1)-c)\Gamma(K-i-r-1)}\,_0F_1\left(2;\frac{(1-z^{-1})K(r+1)}{K(r+1)+(c+1)}\right)\right\}, \quad (91)$$

which directly leads to the expression for the PDF given by (49).

REFERENCES

[1] ECC REPORT 205, "Licensed Shared Access (LSA)," ECC, Tech. Rep., February 2014.

[2] E. Biglieri, "Spectrum sensing," in *Principles of Cognitive Radio*, A. J. Goldsmith, L. J. Greenstein, N. B. Mandayam, and H. V. Poor, Eds. Cambridge University Press, 2012, pp. 150–183.

[3] Y. Zeng, C. L. Koh, and Y.-C. Liang, "Maximum eigenvalue detection: theory and application," in *IEEE International Conference on Communications (ICC'08)*, 2008, pp. 4160–4164.

[4] Y. Zeng and Y.-C. Liang, "Eigenvalue-based spectrum sensing algorithms for cognitive radio," *IEEE Transactions on Communications*, vol. 57, no. 6, pp. 1784–1793, 2009.

[5] A. Kortun, T. Ratnarajah, M. Sellathurai, C. Zhong, and C. B. Papadis, "On the performance of eigenvalue-based cooperative spectrum sensing for cognitive radio," *IEEE Journal of Selected Topics in Signal Processing*, vol. 5, no. 1, pp. 49–55, 2011.

[6] A. Kortun, T. Ratnarajah, M. Sellathurai, Y. Liang, and Y. Zeng, "On the eigenvalue-based spectrum sensing and secondary user throughput," *IEEE Transactions on Vehicular Technology*, vol. 63, no. 3, pp. 1480–1486, 2014.

[7] A. Kortun, T. Ratnarajah, M. Sellathurai, Y.-C. Liang, and Y. Zeng, "Throughput analysis using eigenvalue based spectrum sensing under noise uncertainty," in *Proc. 8th International Wireless Communications and Mobile Computing Conference (IWCMC)*, 2012, pp. 395–400.

[8] E. H. Gismalla and E. Alsusa, "Performance analysis of the periodogram-based energy detector in fading channels," *IEEE Transactions on Signal Processing*, vol. 59, no. 8, pp. 3712–3721, 2011.

[9] ——, "On the performance of energy detection using bartlett's estimate for spectrum sensing in cognitive radio systems," *IEEE Transactions on Signal Processing*, vol. 60, no. 7, pp. 3394–3404, 2012.

[10] ——, "On the detection of unknown signals using Welch overlapped segmented averaging method," in *Proc. IEEE Vehicular Technology Conference (VTC Fall)*, 2011, pp. 1–5.

[11] E. Gismalla and E. Alsusa, "New and accurate results on the performance of the multitaper-based detector," in *Proc. IEEE International Conference on Communications (ICC'12),*, June 2012, pp. 1609–1613.

[12] G. Fikioris, "Integral evaluation using the mellin transform and generalized hypergeometric functions: Tutorial and applications to antenna problems," *IEEE Transactions on Antennas and Propagation*, vol. 54, no. 12, pp. 3895–3907.

[13] ——, *Mellin Transform Method for Integral Evaluation: Introduction and Applications to Electromagnetics (Synthesis Lectures on Computational Electromagnetics)*. Morgan and Claypool Publishers, 2007.

[14] C. Fox, "Some applications of mellin transforms to the theory of bivariate statistical distributions," *Mathematical Proceedings of the Cambridge Philosophical Society*, vol. 53, no. 03, pp. 620–628, 1957.

[15] S. Atapattu, C. Tellambura, and H. Jiang, "Energy detection based cooperative spectrum sensing in cognitive radio networks," *IEEE Transactions on Wireless Communications*, vol. 10, no. 4, pp. 1232–1241, 2011.

[16] V. Garg, *Wireless Communications and Networking*. Elsevier, 2007.

[17] J. Norman and S. Kotz, *Distributions in Statistics: Continuous Univariate Distributions. Vol 2*. New York, US: Wiley, 1970.

[18] R. Tandra and A. Sahai, "SNR walls for signal detection," *IEEE Journal of Selected Topics in Signal Processing*, vol. 2, no. 1, pp. 4–17, 2008.

[19] R. J. Vaughan and W. N. Venables, "Permanent expressions for order statistic densities," *Journal of the Royal Statistical Society. Series B (Methodological)*, pp. 308–310, 1972.

[20] H. A. David and H. N. Nagaraja, *Order Statistics*. John Wiley & Sons, Inc., 2004.

[21] M. K. Simon, *Probability distributions involving Gaussian random variables: A handbook for engineers and scientists.* Springer, 2007.

[22] H.-C. Yang and M.-S. Alouini, *Order Statistics in Wireless Communications.* Cambridge CB2 8RU, UK: Cambridge University Press, 2011.

[23] K. Subrahmaniam, "On some applications of mellin transforms to statistics: Dependent random variables," *SIAM Journal on Applied Mathematics*, vol. 19, no. 4, pp. 658–662, 1970.

[24] M. D. Springer, *The algebra of random variables.* New York, US: Wiley, 1979.

[25] M. D. Springer and W. E. Thompson, "The distribution of products of independent random variables," *SIAM Journal on Applied Mathematics*, vol. 14, no. 3, pp. 511–526, 1966.

[26] I. S. Reed, "The mellin type of double integral," *Duke Mathematical Journal*, vol. 11, no. 3, pp. 565–572, 1944.

[27] A. Sahai and D. Cabric, "A tutorial on spectrum sensing: Fundamental limits and practical challenges," IEEE International Symposium on New Frontiers in Dynamic Spectrum Access Networks (DYSPAN), Nov 2005.

[28] F. Oberhettinger, *Tables of Mellin transforms.* Springer, 1974, vol. 275.

[29] I. S. Gradshteyn and I. M. Ryzhik, *Table of integrals, series, and products*, 7th ed., A. Jeffrey and D. Zwillinger, Eds. New York, USA: Academic Press, 1965, vol. 6.

[30] H. Bateman, A. Erdélyi, H. van Haeringen, and L. P. Kok, *Tables of integral transforms.* New York, USA: McGraw-Hill, 1954, vol. 1.
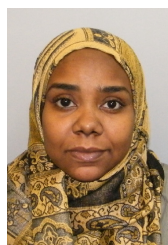
Ebtihal Yousif (S'10-M'13), received the B.Sc. degree with Honours in Electronic Engineering in 2003 and the M.Sc. degree in 2007 from Sudan University of Science and Technology (SUST). From 2005 to June 2007 she served as a teaching assistant and then she worked as a lecturer till December 2008 in the Electronic Engineering department in SUST. In 2009, She joined the Microwave and Communications Systems (MACS) group of the University of Manchester where she worked as part-time staff and received her P.hD degree in 2013. She is currently a research fellow within the FP7 project ADEL (3.7M€) in the area of licensed shared access. Her primary research interests are in wireless communication systems including next generation technologies, dynamic spectrum access, statistical signal processing, information theoretic aspects, MIMO systems and applications of machine learning for wireless systems.

Tharmalingam Ratnarajah (A'96-M'05-SM'05) is currently with the Institute for Digital Communications, University of Edinburgh, Edinburgh, UK, as a Professor in Digital communications and signal processing. His research interests include signal processing and information theoretic aspects of 5G wireless networks, full-duplex radio, mmWave communications, random matrices theory, interference alignment, statistical and array signal processing and quantum information theory. He has published over 250 publications in these areas and holds four U.S. patents. He is currently the coordinator of the FP7 projects HARP (3.2M€) in the area of highly distributed MIMO and ADEL (3.7M€) in the area of licensed shared access. Previously, he was the coordinator of FP7 Future and Emerging Technologies project CROWN (2.3M€) in the area of cognitive radio networks and HIATUS (2.7M€) in the area of interference alignment. Dr Ratnarajah is a Fellow of Higher Education Academy (FHEA), U.K., and an associate editor of the IEEE Transactions on Signal Processing.

Mathini Sellathurai (S'95-M'02-SM'06) is presently a Reader with the Heriot-Watt University, Edinburgh, U.K and leading research in signal processing for intelligent systems and wireless communications. Her research includes adaptive, cognitive and statistical signal processing techniques in a range of applications including Radar and RF networks, Network Coding, Cognitive Radio, MIMO signal processing, satellite communications and ESPAR antenna communications. She has been active in the area of signal processing research for the past 15 years and has a strong international track record in multiple-input, multiple-output (MIMO) signal processing with applications in radar and wireless communications research. Dr. Sellathurai has 5 years of industrial research experience. She held positions with Bell-Laboratories, New Jersey, USA, as a visiting researcher (2000); and with the Canadian (Government) Communications Research Centre, Ottawa Canada as a Senior Research Scientist (2001-2004). Since 2004 August, she has been with academia. She also holds an honorary Adjunct/Associate Professorship at McMaster University, Ontario, Canada, and an Associate Editorship for the IEEE Transactions on Signal Processing between 2009 -2013 and presently serving as an IEEE SPCOM Technical Committee member. She has published over 150 peer reviewed papers in leading international journals and IEEE conferences; given invited talks and written several book chapters as well as a research monograph titled Space-Time Layered Processing as a lead author. The significance of her accomplishments is recognized through international awards, including an IEEE Communication Society Fred W. Ellersick Best Paper Award in 2005, Industry Canada Public Service Awards for contributions in science and technology in 2005 and awards for contributions to technology Transfer to industries in 2004. Dr. Sellathurai was the recipient of the Natural Sciences and Engineering Research Council of Canadas doctoral award for her Ph.D. dissertation.
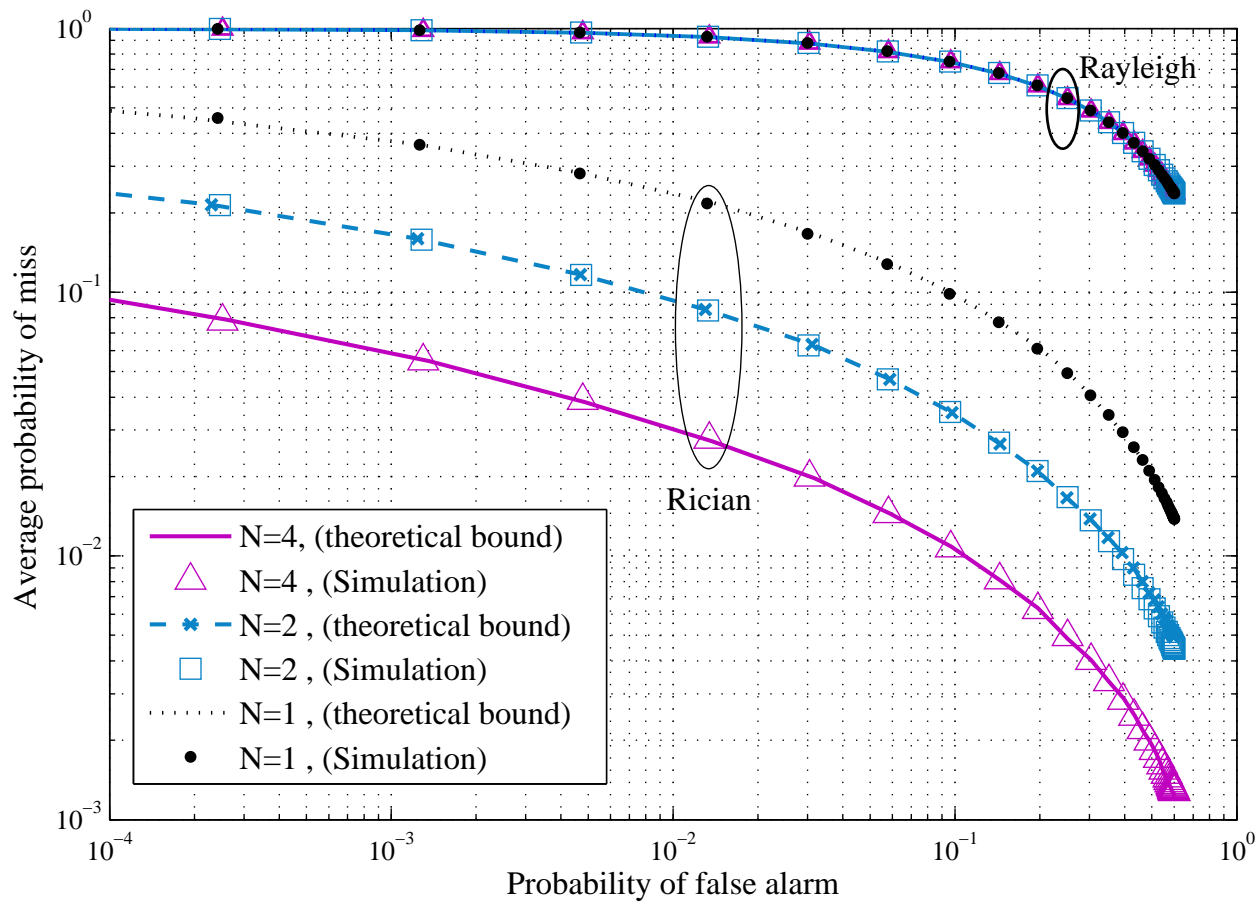
Fig. 1. Complementary receiver operating characteristic curves for MED with various cases of number of antenna branches N. ($M = 16$, $K = 2$, $\sigma_s^2 = -3$dB, $\sigma_w^2 = 0$dB, $\sigma_h^2 = 0$dB, $|\mu_h|^2 = 13$)
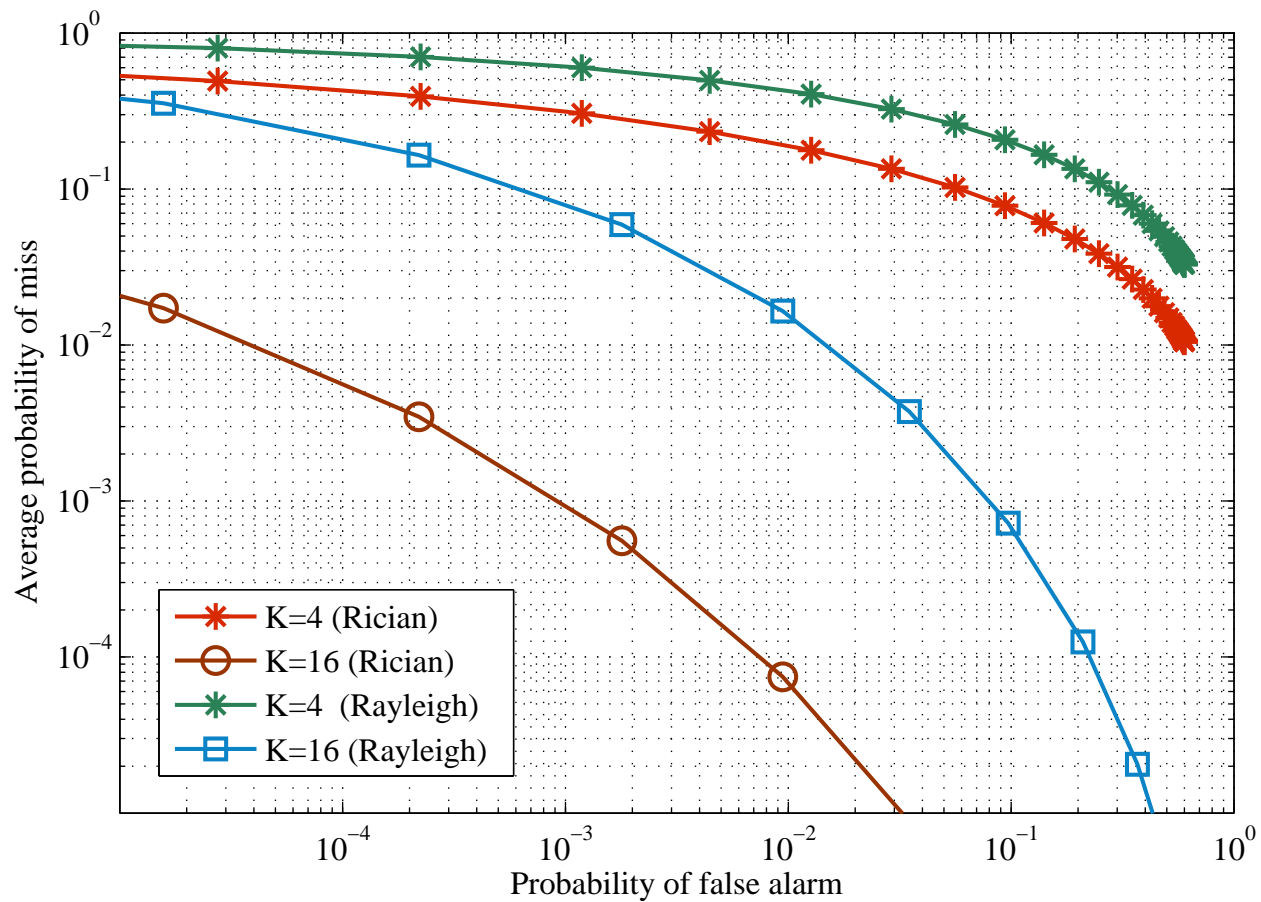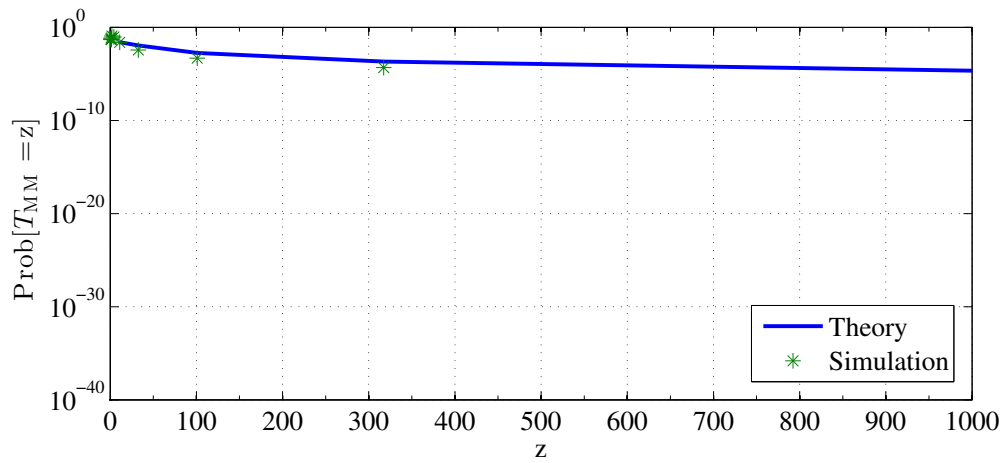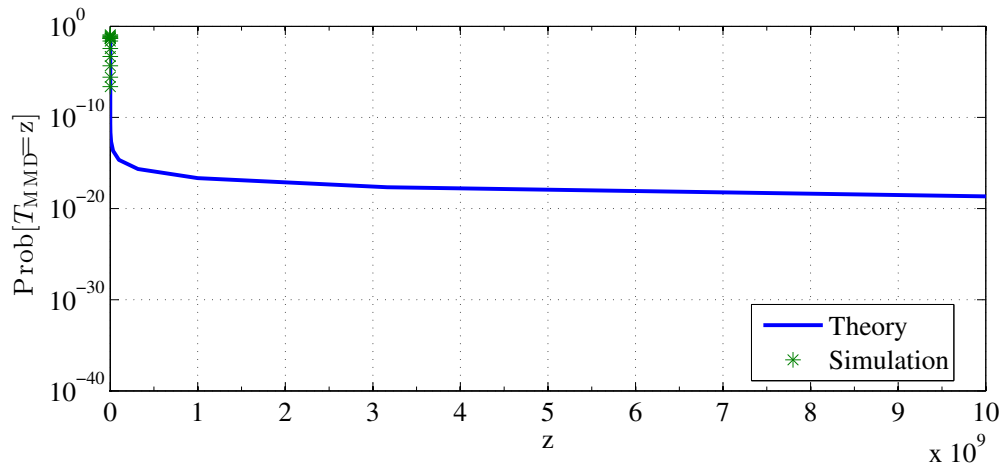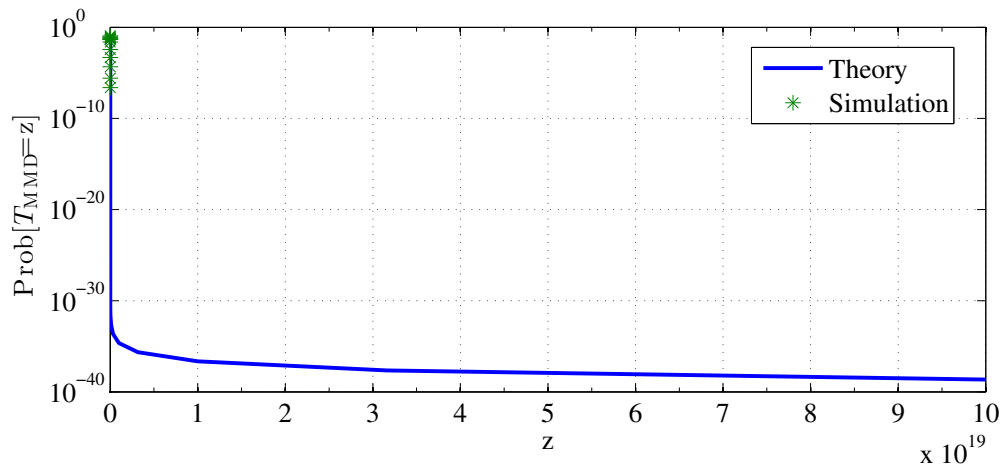
Fig. 2. Impact of number of sensing sub-slots for MED ($M = 1024$, $N = 4$, $\sigma_w^2 = 0$dB, $\sigma_s^2 = -6$dB, $\sigma_h^2 = 0$dB, $|\mu_h|^2 = 4$).

(a) Case I

(b) Case II

(c) Case III

Fig. 3. Illustration of the Heavy tailed properties of the PDF of T_{MME}

(a) Rayleigh

(b) Rician
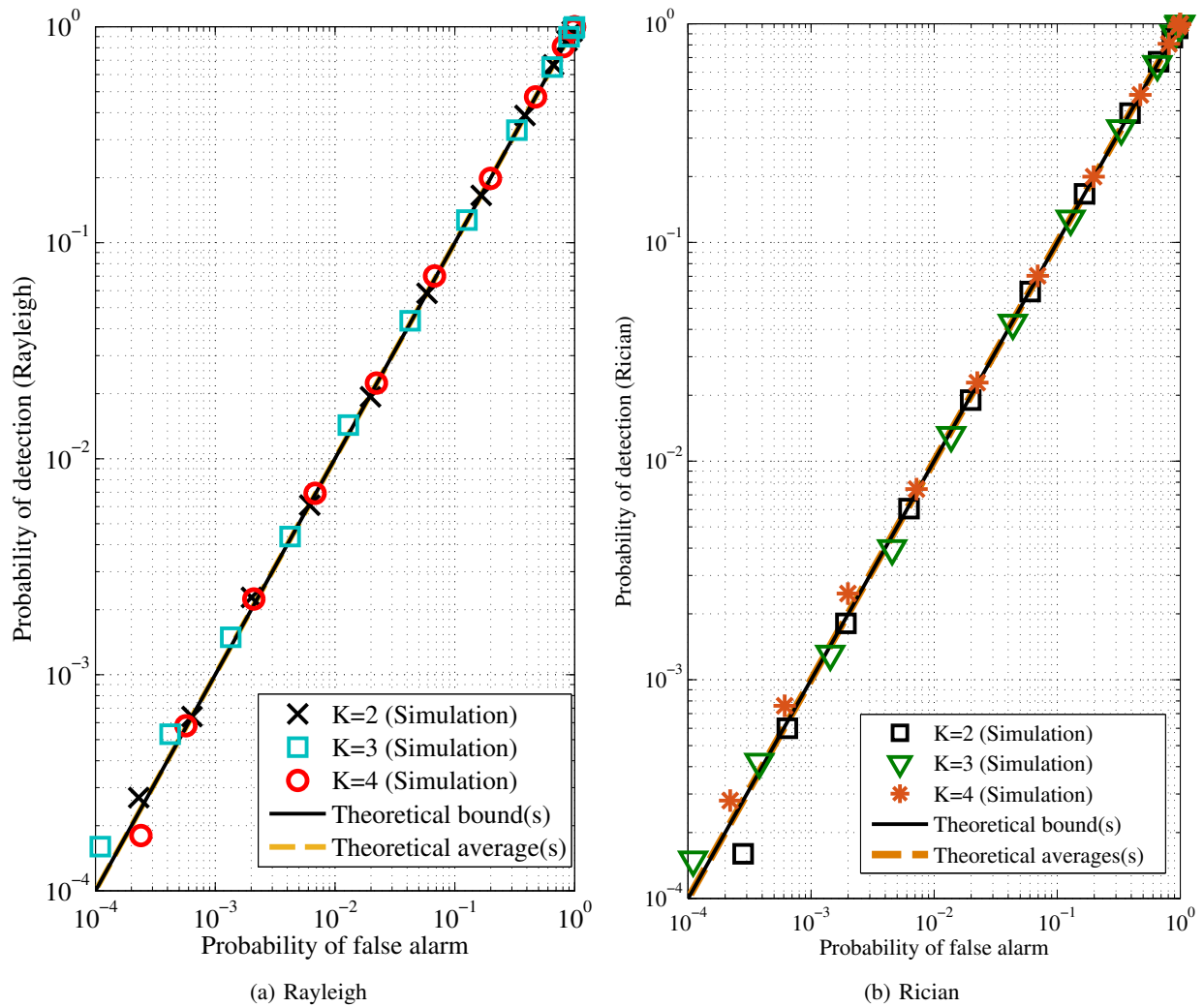
Fig. 4. Receiver operating characteristic curves for the maximum-minimum eigenvalue detector
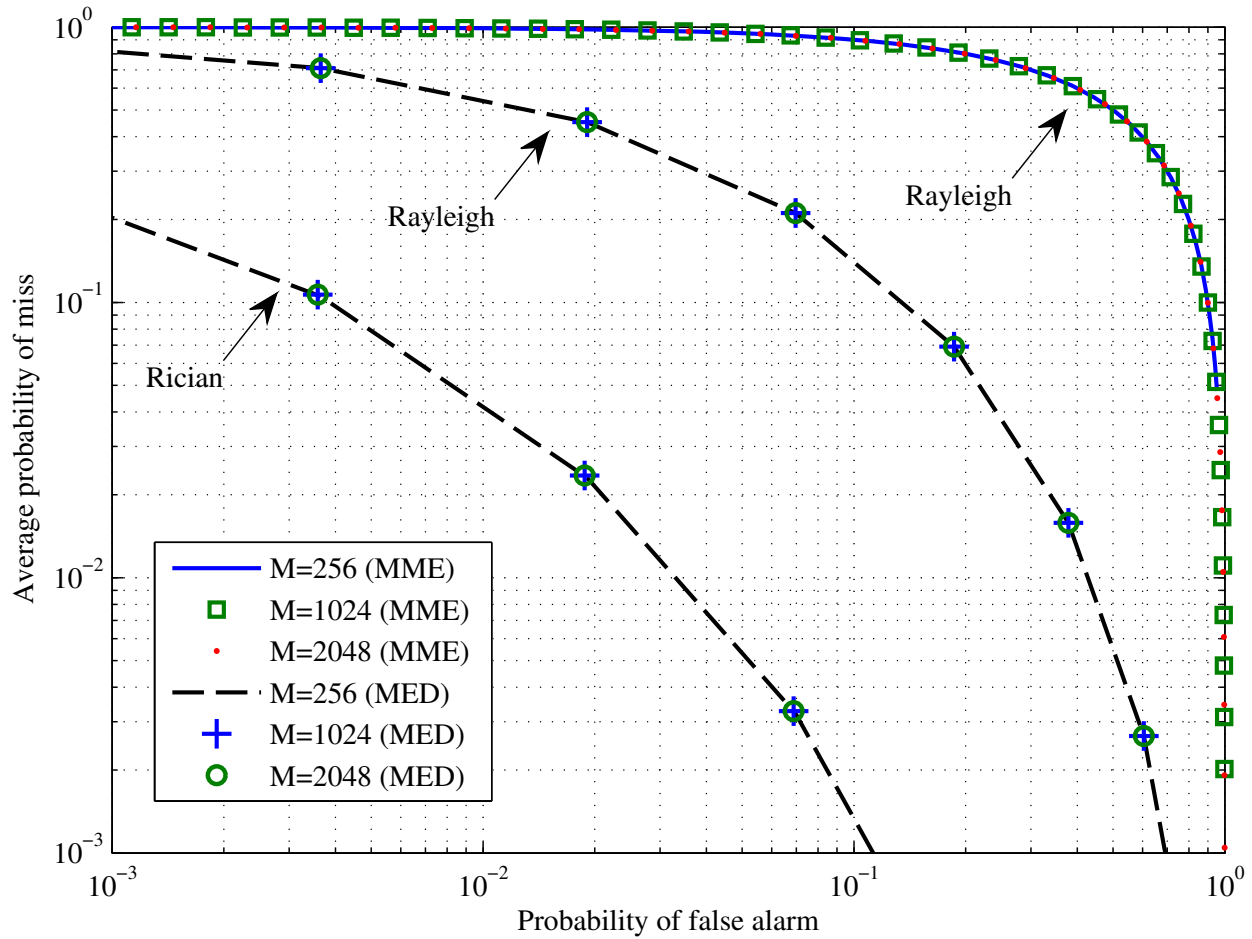
Fig. 5. Comparison between MED and MME based on impact of fixed number of sensing slots and varied total frame length
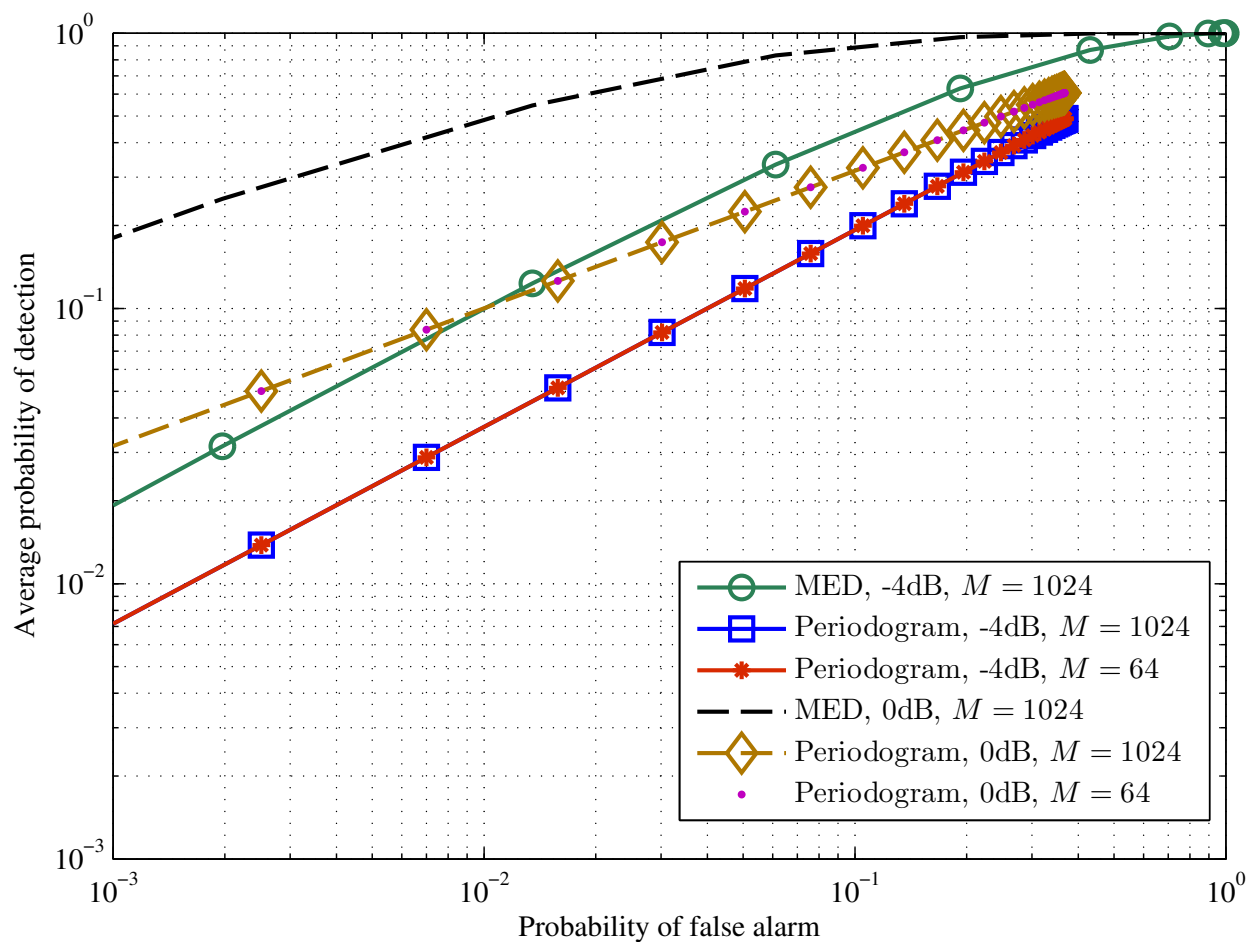
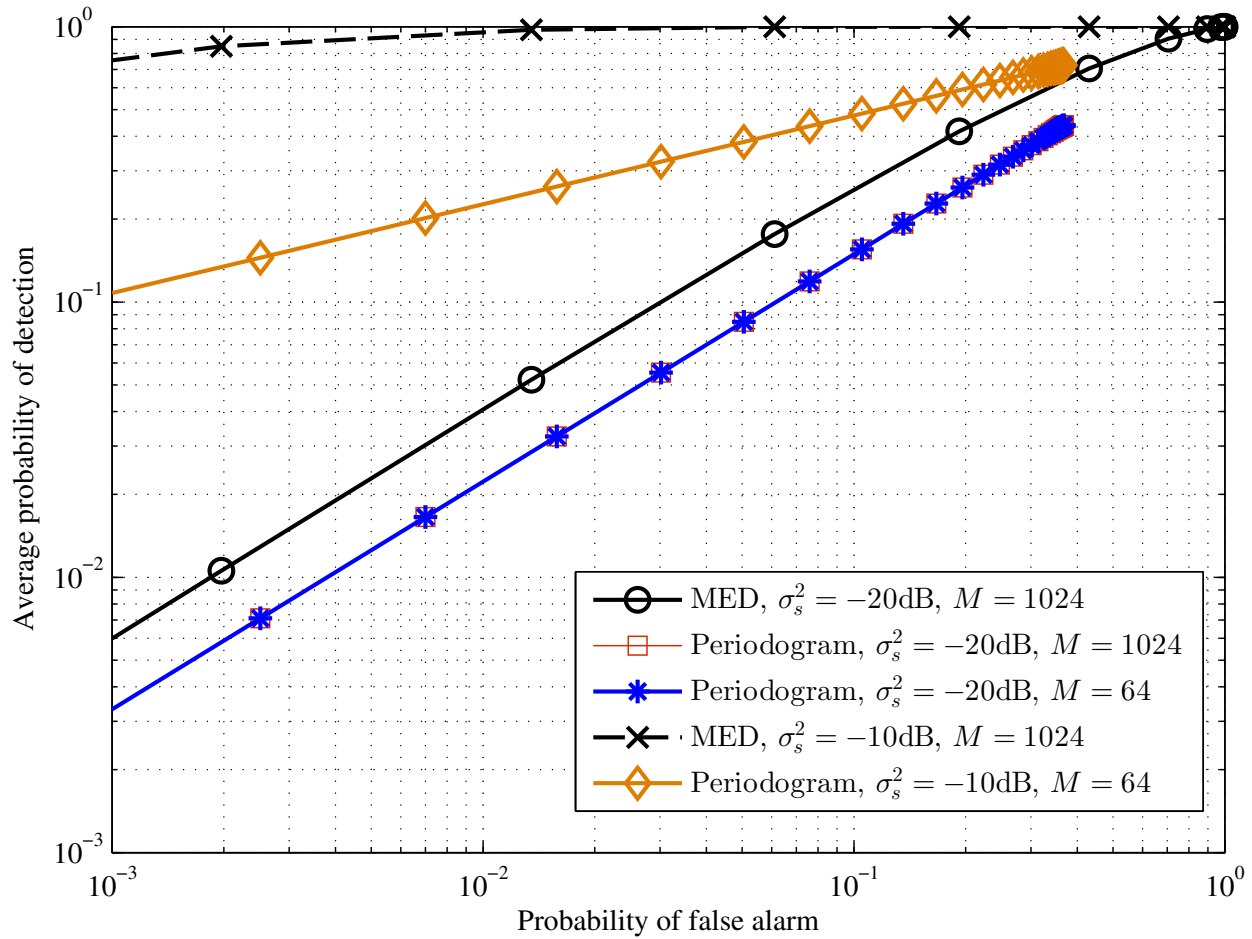Fig. 6. Impact of noise uncertainty over Rayleigh fading

Fig. 7. Impact of noise uncertainty over Rician fading ($\mathbb{E}[|\mu_h^2|^2] = 4.5$)